BNL-NUREG -31290
INFORMAL REPORT

LIMITED DISTRIBUTION

SIMULATION OF ZION UNIT 2

CYCLE-1 OPERATION

P. Kohut, D. Cokinos and J. Carew

Core Performance Group

DEPARTMENT OF NUCLEAR ENERGY BROOKHAVEN NATIONAL LABORATORY
UPTON, NEW YORK 11973

Prepared for the U.S. Nuclear Regulatory Commission
Office of Nuclear Reactor Regulation
Contract No. DE-AC02-76CH00016

BNL-NUREG-31290
INFORMAL REPORT
LIMITED DISTRIBUTION

SIMULATION OF ZION UNIT 2

CYCLE-1 OPERATION

P. Kohut, D. Cokinos and J. Carew

Core Performance Group

April 1982

Core Performance Group
Department of Nuclear Energy
Brookhaven National Laboratory
Upton, New York, 11973

Prepared for
U.S. Nuclear Regulatory Commission
Washington, D.C. 20555
Under Interagency Agreement DE-AC02-76CH00016
NRC FIN. No.A-3374

NOTICE: This document contains preliminary information and was prepared primarily for interim use. Since it may be subject to revision or correction and does not represent a final report, it should not be cited as reference without the expressed consent of the author(s)

ACKNOWLEDGMENTS

The authors would like to thank A. Aronson of BNL for making the computer programming changes and providing valuable assistance during the course of this work. The typing was expertly done by L. Ryan.

The work was performed under the auspicies of the U.S. Nuclear Regulatory Commission, Marvin Dunenfeld, Technical Monitor.

TABLE OF CONTENTS

List of Figures

LIST OF TABLES

1.0 INTRODUCTION

The work summarized in this report was performed to (a) further expand the capability for simulating incore conditions of a pressurized water reactor (PWR) at BNL, (b) benchmark specific code modules and (c) compile additional nuclear data for static and transient analysis. This effort is intended to provide the data-base for wide ranging on-call technical assistance to the U.S. Nuclear Regulatory Commission. Previous efforts by BNL to simulate static core behavior have included core follow analyses of the H. B. Robinson (PWR) Cycle 1, [1] and Quad Cities (BWR) Cycles 1 and 2. [2,3]

In three-dimensional steady state reactor analysis two basic calculational tools are used; (1) a two-dimensional fuel assembly code which generates nuclear data (cross sections, k_∞ , M^2 etc.) for every fuel type in the core and (2) a three-dimensional coupled neutronics/thermal-hydraulics code which simulates the core behavior by simultaneous solution of the power, exposure, temperature and xenon distributions and effective multiplication factor.

Zion Unit 2, a four loop Westinghouse (W) PWR design, was chosen because of the number of similar plants expected to be operating in the next several years and the large volume of Zion-2 core design and operating data that is available.[4] These reference quality data constitute a substantial data base for validating any PWR core analysis methodology. Comparison of calculation to measurements of core power distributions and core responses during certain operational maneuvers are included in this report.

The simulation of Zion Unit 2 operation has been carried out with the CASMO fuel assembly code and the three-dimensional reactor code, NODE-P. Thermal-hydraulic analysis was performed separately with THERM-P, another ARMP code module.

Detailed core parameters have been obtained at each of the 23 state points spanning Cycle-1. At each state point the calculated and measured relative (axially integrated) assembly powers have been compared.

A description of the physics methodology used in the codes is briefly discussed in chapter 2. Design and measured data, operating characteristics, input information and data generation are presented in Chapter 3. Results and comparison with measured data are shown and discussed in Chapter 4. Appendix A presents a comparison of 15x15 and 17x17 (W optimized design) fuel assemblies while Appendix B lists the "B" - constants used in the present study.

2.0 METHODOLOGY

The simulation of PWR core operation requires the solution of the three-dimensional coupled neutronics/thermal-hydraulics reactor equation. As is the usual procedure, the lattice fine structure equations are solved separately providing parametric nuclear data including few group macroscopic and microscopic data, isotopic concentrations, etc. The assembly data are then used in the three-dimensional neutron diffusion calculation to compute core-wide power, exposure, and temperature distributions as well as reactivity for a given set of operating conditions. The lattice physics calculations were performed with the CASMO code and the global reactor core analysis with the nodal code, NODE-P. A simplified block diagram showing data flow among the various calculational modules is shown in Fig. 2.1.

2.1 Lattice Physics Analysis-CASMO

The fuel assembly calculations were performed with the multigroup two-dimensional transport theory code, CASMO[5]. The code, developed by Studsvik, analyzes fuel assemblies with cylindrical fuel rods of varying compositions arranged in a square array. The block diagram of the calculational sequence of CASMO is shown in Fig. 2.2.

The code uses a 69 group microscopic cross section library, which is based on ENDF-B/III. A special module is used for the calculation of the effective cross sections in the resonance region for important resonance absorbers. The heterogeneous problem is related to an equivalent homogeneous problem through the use of the resonance equivalence theorem. Effective absorption and fission cross sections are calculated from the resonance integrals which have been obtained from the equivalence expressions. A correction is made for the interaction effects arising from the presence of more than one resonance absorber and the spatial screening effects are taken into account by the Dancoff-factors. A 69-group infinite medium spectrum is calculated then, using the method of collision probabilities, for each different type of fuel pin. The 69-group spectra are used to obtain 12 broad-group cross sections for the succeeding calculations. The two-dimensional transmission probablility analysis performed in 12 groups, yields a detailed flux distribution in the fuel assembly as well as the multiplication factor (eigenvalue). The average few group cross sections and reaction rates are generated by using the final flux distribution.

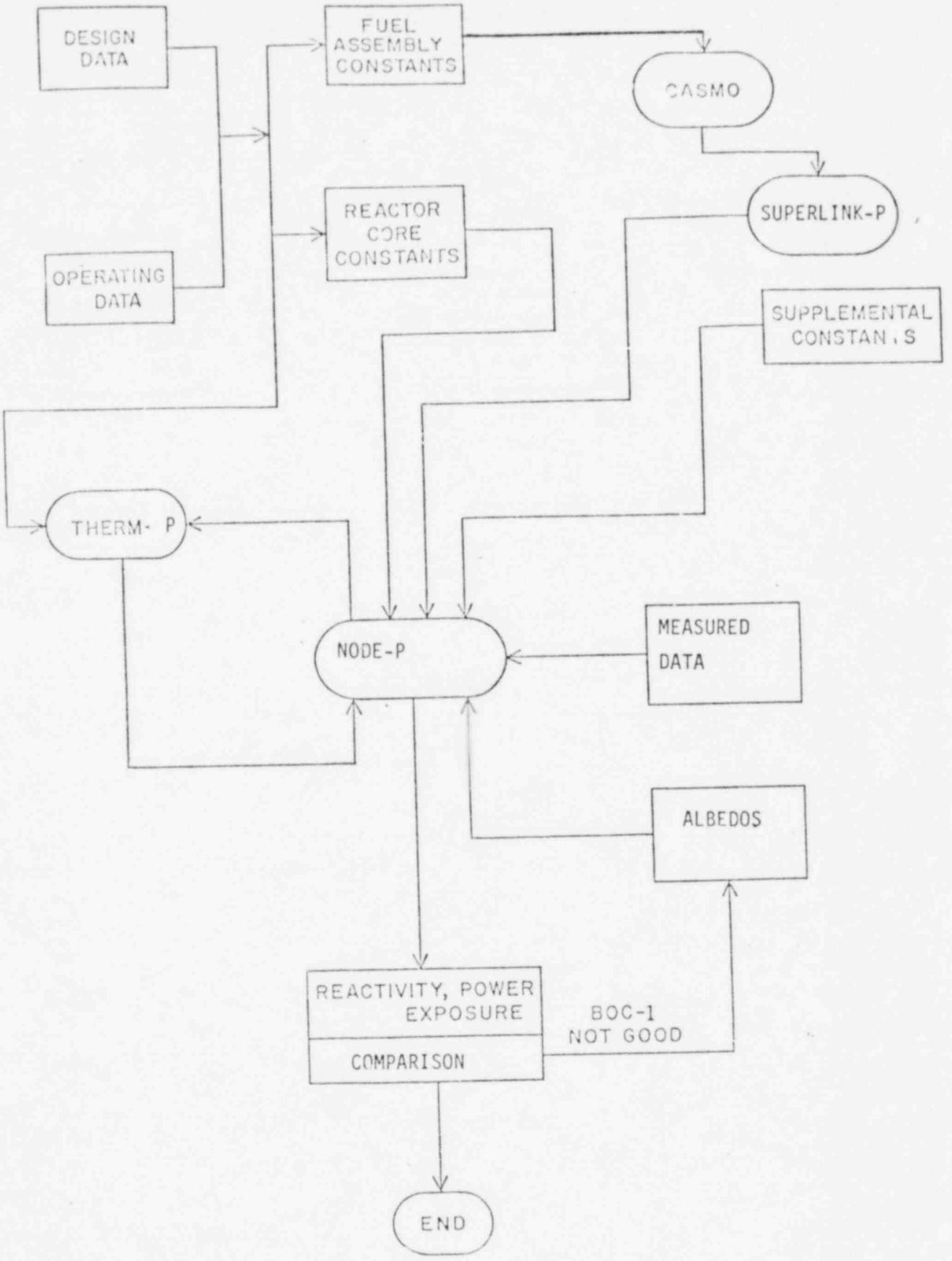

Fig. 2.1 Data Flow in Simulation of Zion Unit 2, Cycle-1

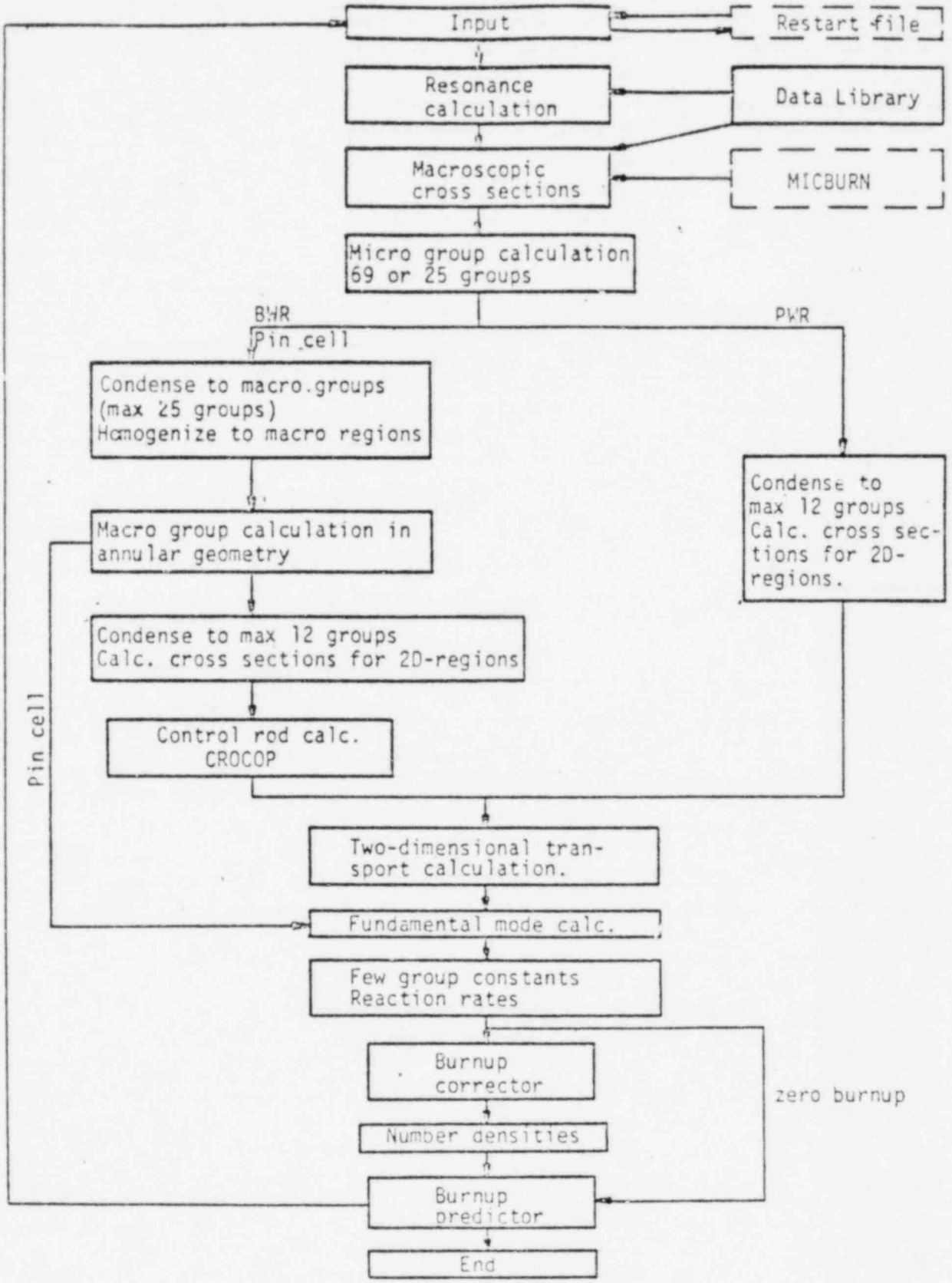

Figure 2.2 CASMO flow diagram

2.2 Reactor Core Calculations-NODE-P

The global reactor analysis is performed by NODE-P[6], which computes the core effective multiplication factor and the three-dimensional core power, exposure, coolant flow and temperature distributions. The effects of partially inserted full-length control rods and part-length rods are explicitly treated. The code is capable of handling 13 different fuel types constituting the core loading. Each fuel bundle is uniquely represented and divided into 12 axial segments or, nodes.

The nodal infinite multiplication factor, k_∞ , and migration area, M^2, are the basis for calculating the local neutron source, power and reactivities. The core wide effective multiplication factor, k_{eff}, is computed using the same parameters. The nodal k_∞ and M^2 values are obtained from the lattice physics, CASMO calculations as a function of enrichment, burnable poison content, coolant and fuel temperature, boron concentration and control rod position. The program iterates to account for the interaction between power distribution and core nuclear properties which depend on coolant flow, coolant and fuel temperature and xenon distribution. For an initial distribution of coolant temperature, fuel temperature, xenon and fuel exposure, the power and core k_{eff} are first converged. New coolant temperature, Doppler effect and xenon distributions are established consistent with the converged source. This power-coolant temperature iteration is repeated until the nuclear properties and power-temperature distributions have converged to consistent values within an input error criterion. The fuel exposure distribution is then extended to the end of step and the sequence of source, temperature and xenon convergence is repeated. The block diagram showing the interaction between power and nuclear properties in NODE-P is shown in Fig. 2.3. Operating conditions such as thermal reactor power, core flow, inlet subcooling, core pressure and control rod positions are introduced as basic input data. The channel inlet flow as a function of assembly power distribution is obtained from the THERM-P Program.

2.3 Thermal-hydraulics Calculations - THERM-P

The channel flow distribution required by NODE-P as input data, is calculated by another ARMP code module, THERM-P[7]. The program calculates the flow, temperature, enthalpy and void distributions in a pressurized water reactor core and determines the thermal performance of the fuel. The input includes thermal reactor power level, power distribution (from NODE-P), flow channel configuration, total coolant flow, pump head and loss coefficients. To establish the final channel flow distribution some iteration is needed between THERM-P and NODE-P, because of the core thermal-hydraulic feedback.

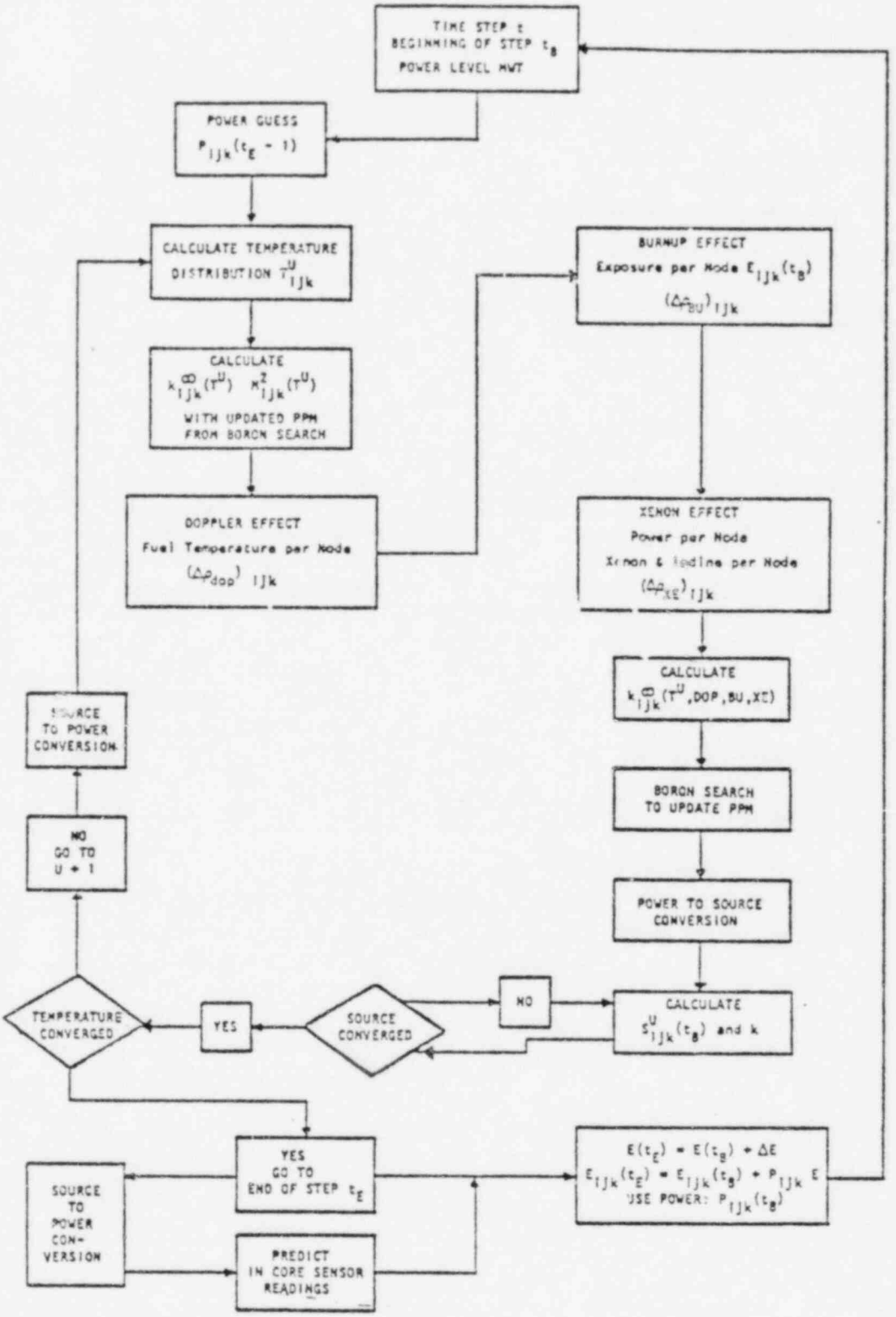

Fig. 2.3 EPRI-NODE-P Flowchart

3.0 CALCULATIONAL MODEL AND DATA GENERATION

The principal source of information necessary for carrying out our calculation has been Reference 4. Fuel assembly data and certain operating characteristics were the main input required for CASMO. Core design and operating data as well as data generated by CASMO and processed by SUPERLINK-P constituted the input base for NODE-P. The channel flow distribution obtained from THERM-P was also input.

3.1 Design And Operating Data

Nuclear design parameters for the Zion Unit 2 Cycle 1 core consisting of thermodynamic data, core component description and operating characteristics including measured core physics parameters and detailed operating histories with corresponding power distributions have been carefully documented in Reference 4.

3.1.1 Fuel Assembly Data

The Zion 2, cycle-1, core contained 193 fuel assemblies. The bundles are in a 15x15 rod array and can be grouped in three distinct categories based on the U^{235} enrichment (Region 1, 2 and 3). Table 3.1a and 3.1b describe the fuel types and also lists assembly design data. In two of the three fuel types (region 2 & 3) further classification may be made based on the number of burnable poison rods (BPR's) contained in the bundle. The fuel assembly consists of 204 fuel rods and 21 water holes. Assemblies with BPR's contain the same number of fuel rods (204) but in place of some of the water holes are borated pyrex-glass rods. Figures 3.1 through 3.3 describe the layout of these assembly types.

3.1.2. Reactor Core Data

As indicated earlier, the Zion Unit-2 contained 193 fuel assemblies. The various design characteristics of the core are shown in Table 3.2. Figure 3.4 shows the reactor core map and the location of the fuel assemblies by regions. The locations of fuel bundles containing burnable poison rods are indicated in Fig. 3.5. Figure 3.6 shows those assemblies where movable detector access has been provided.

The movable detectors play an important role since their responses and the power map which can be derived from these signals, establish the standard which must be matched by the calculation.

TABLE 3.1a

Fuel Assembly Data

Region+	1	2	2	2	2	3	3	3	3	3
Fuel Type	1	2*	3	4*	5	6	7	8	9	10
# Of Assemblies In Core	65	24	24	12	4	8	8	8	12	28
Enrichment (W/o U^{235})	2.25	2.79	2.79	2.79	2.79	3.29	3.29	3.29	3.29	3.29
Geometry	15x15	15x15	15x15	15x15	15x15	15x15	15x15	15x15	15x15	15x15
# Fuel Rods	204	204	204	204	204	204	204	204	204	204
Fuel Rod Pitch, In.	.563	.563	.563	.563	.563	.563	.563	.563	.563	.563
Assembly Pitch, In.	8.466	8.466	8.466	8.466	8.466	8.466	8.466	8.466	8.466	8.466
Instrument Location	1	1	1	1	1	1	1	1	1	1
Water Rods	20	0	4	8	20	0	8	12	11	20
Burnable Poison Rods	0	20	16	12	0	20	12	8	9	0

*Including Special Source Assemblies

+ See Also Fig. 3.4.

TABLE 3.1b

Fuel Assembly Data

Fuel Rod

Fuel Pellet Material/Density	Region 1	sintered UO_2/10.28 g/cm^3
	Region 2	sintered UO_2/10.17 g/cm^3
	Region 3	sintered UO_2/10.32 g/cm^3
Cladding Material/Density		Zircaloy-4/1.284 g/cm
Cladding I.D., cm		0.9486
Cladding O.D., cm		1.072

Guide Tube

Guide Tube Material	Zircaloy-4
Guide Tube I.D., cm	1.308
Guide Tube O.D., cm	1.384

Burnable Poison Rod (BPR)

Rod Material	Borosilicate Glass
Natural Boron Loading	0.0603 g/cm
Cladding Material (Inner-Outer)	SS 304
Inner Clad I.D., cm	0.568
Inner Clad O.D., cm	0.601
Outer Clad I.D., cm	1.077
Outer Clad O.D., cm	1.116

Rod Cluster Control

Rod Material	5% Cd-15% In-80% Ag
Clad Material	SS 304
Clad Thickness, cm	0.124

FUELS WITHOUT BURNABLE ABSORBER RODS

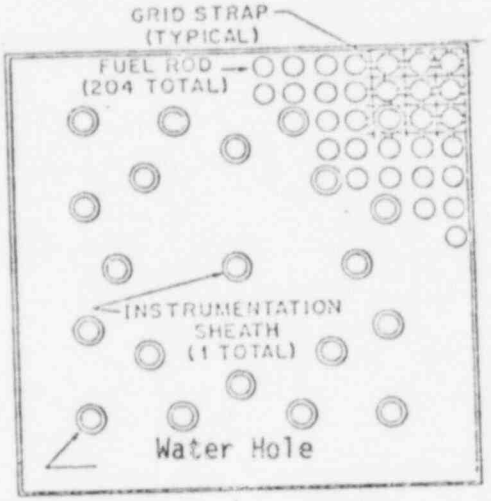

Fuel Type I	
Region	1
Enrichment (w/o)	2.248
BPR	0
Water Hole (Control Rod Location)	20

Fuel Type 10	
Region	3
Enrichment (w/o)	3.292
BPR	0
Water Hole	20

Fig. 3.1 Zion Unit 2 Fuel Types
Fuels Without BPR

REGION 2 FUEL ENRICHMENT 2.78%

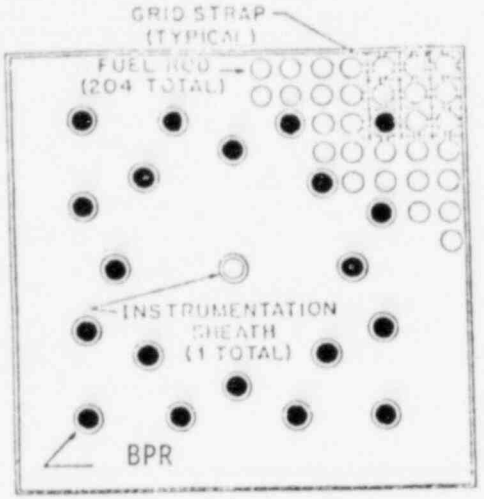

Fuel Type	2
BPR	20
Water Hole	0

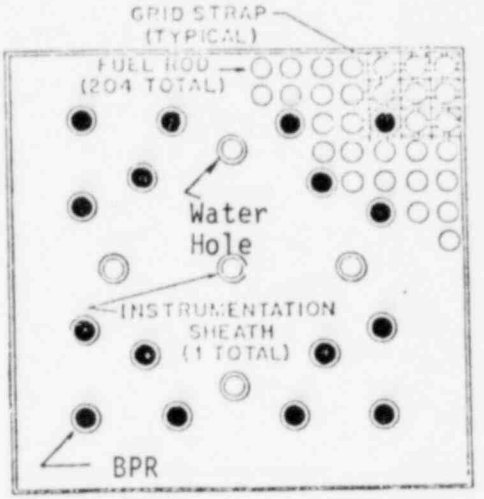

Fuel Type	3
BPR	16
Water Hole	4

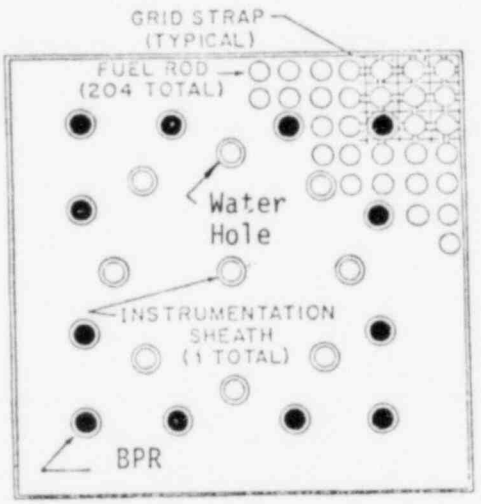

Fuel Type	4
BPR	12
Water Hole	8

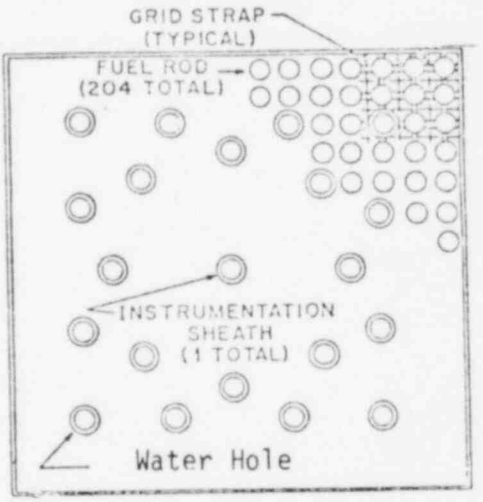

Fuel Type	5
BPR	0
Water Hole	20

Fig. 3.2 Zion Unit 2 Fuel Types, Region 2

Region 3 Fuel Enrichment 3.292%

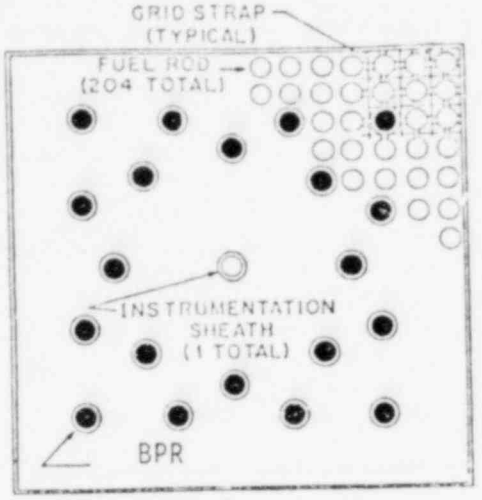

Fuel Type	6
BPR	20
Water Hole	0

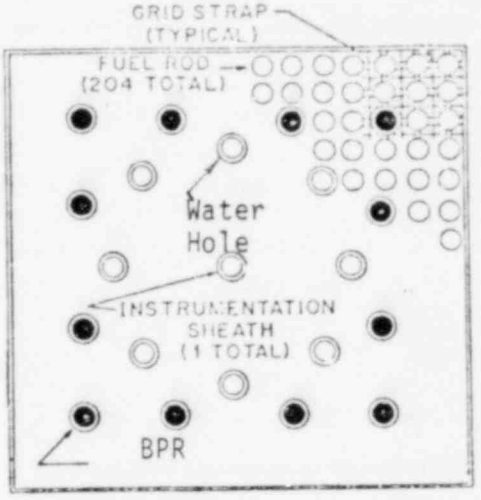

Fuel Type	7
BPR	12
Water Hole	8

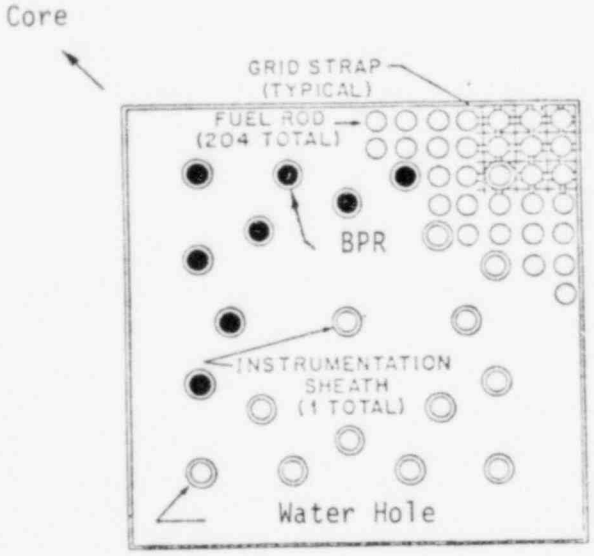

Fuel Type	8
BPR	8
Water Hole	12

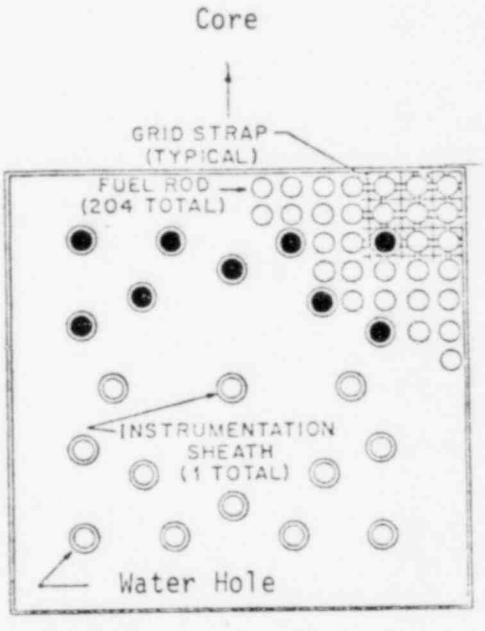

Fuel Type	9
BPR	9
Water Hole	11

Fig. 3.3 Zion Unit 2 Fuel Types, Region 3

TABLE 3.2

Reactor Core Data

Rated core thermal power, MW	3250
Total core flow, kg/hr	6.67×10^7
Volumetric Power Density, KW/	99.9
Linear Power Density, W/cm	226.4
Reactor Coolant Pressure kg/cm^2 (PSIA)	158.23 (2250.)
Total Number of Fuel Assemblies	193
Number of Fuel Assembly Types (Region)	3

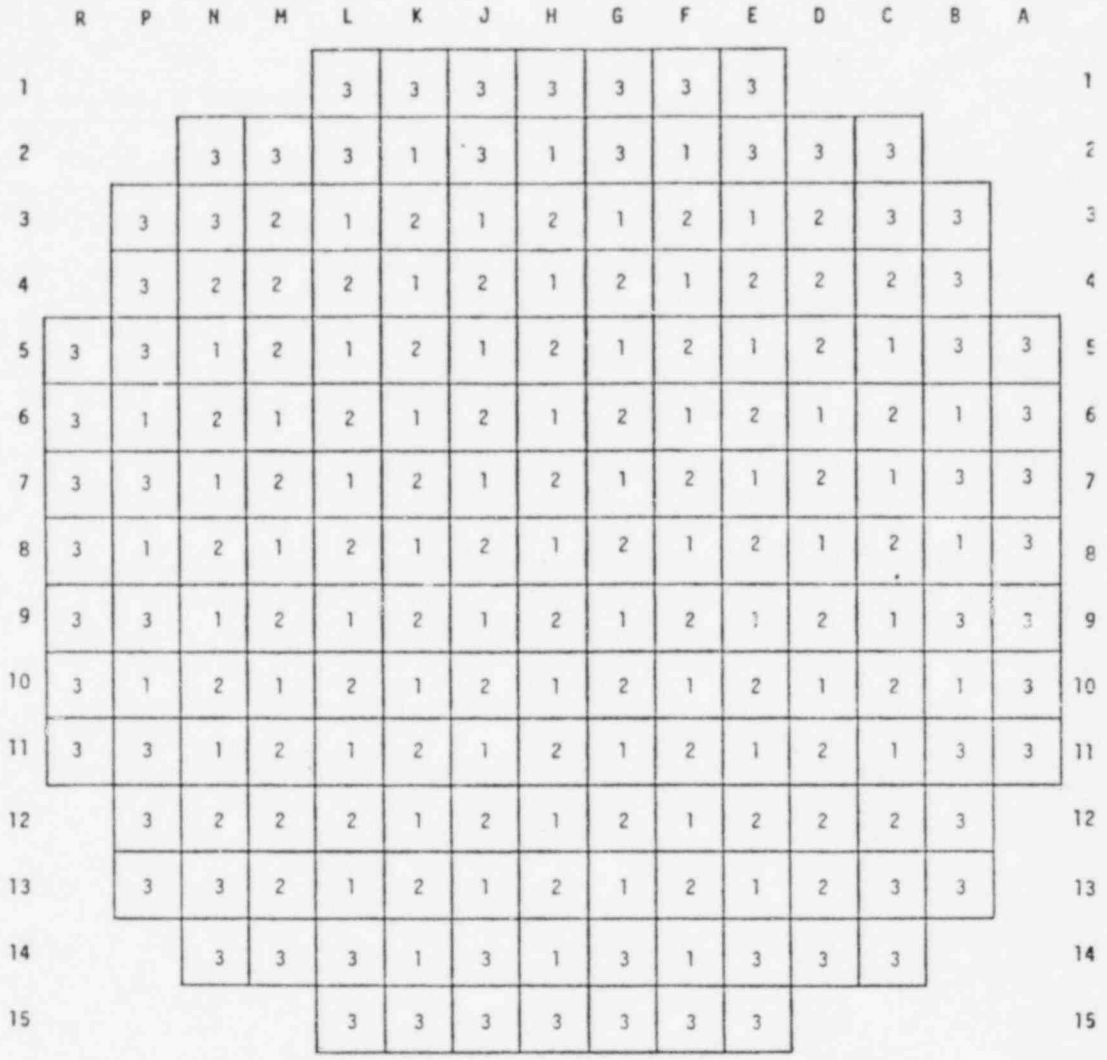

Symbol	Region	Enrichment (w/o)	No. of Assemblies
1	1	2.248	65
2	2	2.789	64
3	3	3.292	64

Fig. 3.4 Location of Fuel Assemblies by Regions

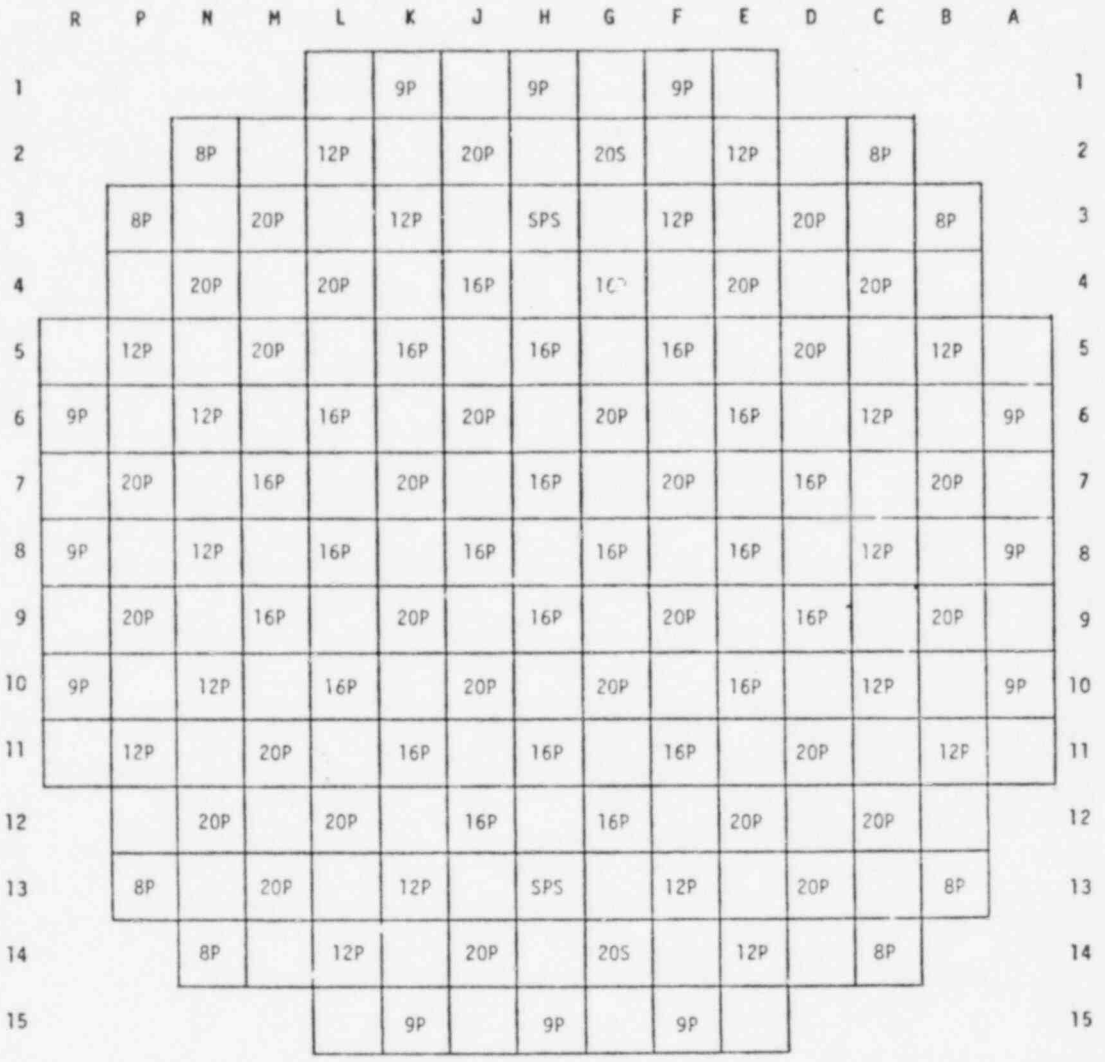

STANDARD ASSEMBLIES

Symbol	# B/P Rods per Insert	# Inserts
20P	20	30
16P	16	24
12P	12	18
9P	9	12
8P	8	8

SPECIAL SOURCE BEARING ASSEMBLIES

Symbol	# B/P Rods per Insert	# Inserts
20S	19	2
SPS	12	2

Fig. 3.5 Location of Fuel Assemblies Containing BPR

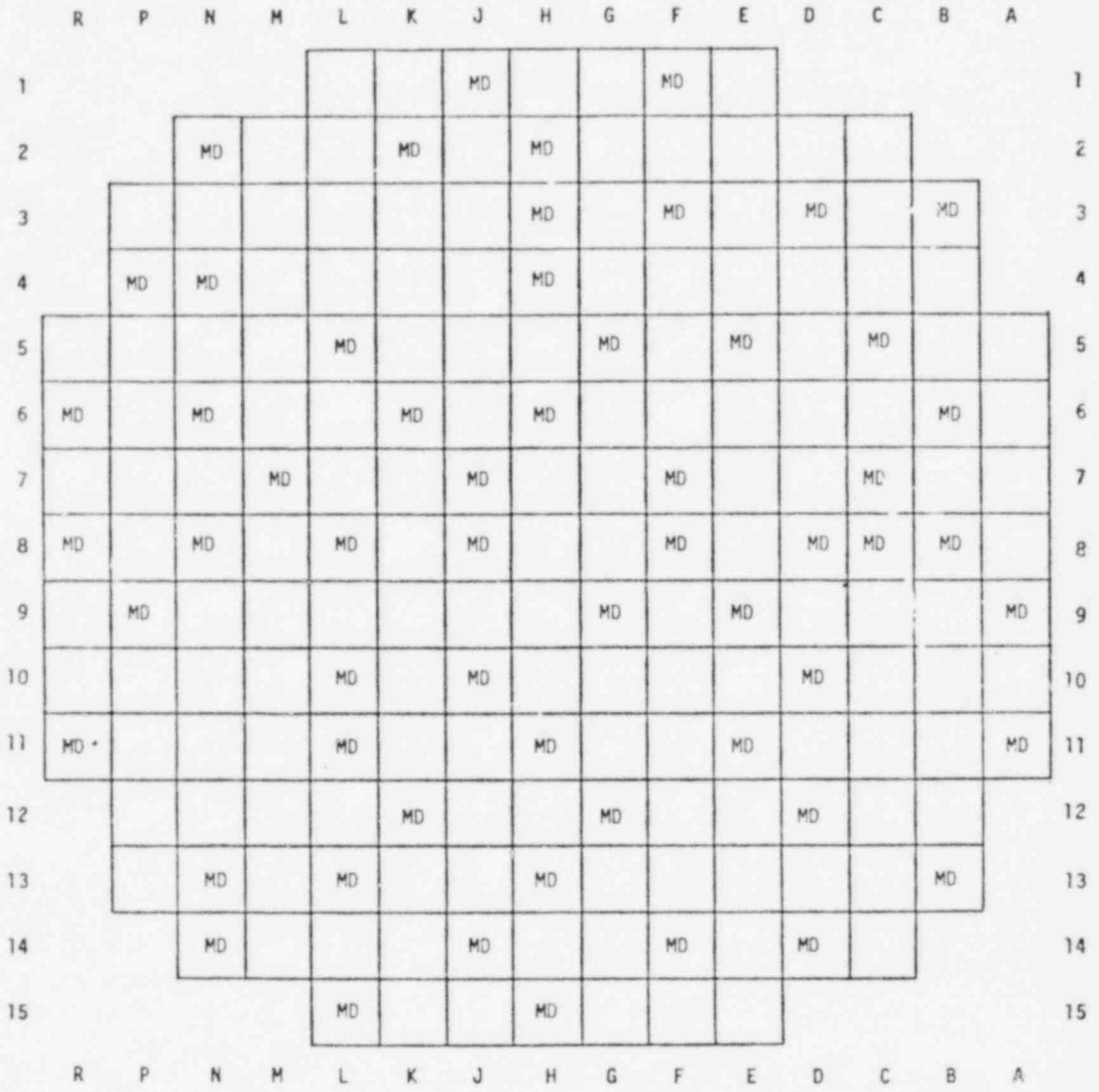

MD = Movable Detector Access Thimble

Fig. 3.6 Locations of Movable Detector Thimbles

3.1.3 Operating Data Measurements

The primary data representing each operating state of the reactor core consisted of:

Core thermal power (including power level changes)
Control bank positions (Bank "D" and "part length")
Reactor coolant pressure
Reactor coolant boron concentration
Core average exposure
Flux maps (Power Distribution)

The scope of our calculations was essentially limited to simulating three major groups of compiled measured data:

1. Relative region-wise reaction rate integrals (Detector Responses)

2. Inferred relative assembly power distribution

3. Core average axial power distribution

A sample of typical data sets showing the radial detector and power core distributions are shown in Fig. 3.7 and 3.8 respectively. A sample of the core average axial conditions is shown in Fig. 3.9. There are 23 data sets representing the initial conditions and subsequent operating history of Cycle-1.

3.2 Fuel Assembly Model and Calculations

CASMO calculations have been performed for all initial fuel types with symmetrical fuel rod arrangements (types 1 through 7 and type 10). The BPR's in type 8 and 9 fuels were non-symmetrically loaded (Fig. 3.3), and therefore could not be modelled in the present version of CASMO. These assemblies (Region 3) are located on the periphery where the power is low. Errors made in modelling the asymmetries in these assemblies will not significantly affect the calculational results. In the CASMO calculations, type 8 and 9 fuels were replaced with a symmetric fuel assembly containing 8 BPR's in such a way that the infinite medium geometric arrangement approximated rather closely the non-symmetric configurations.

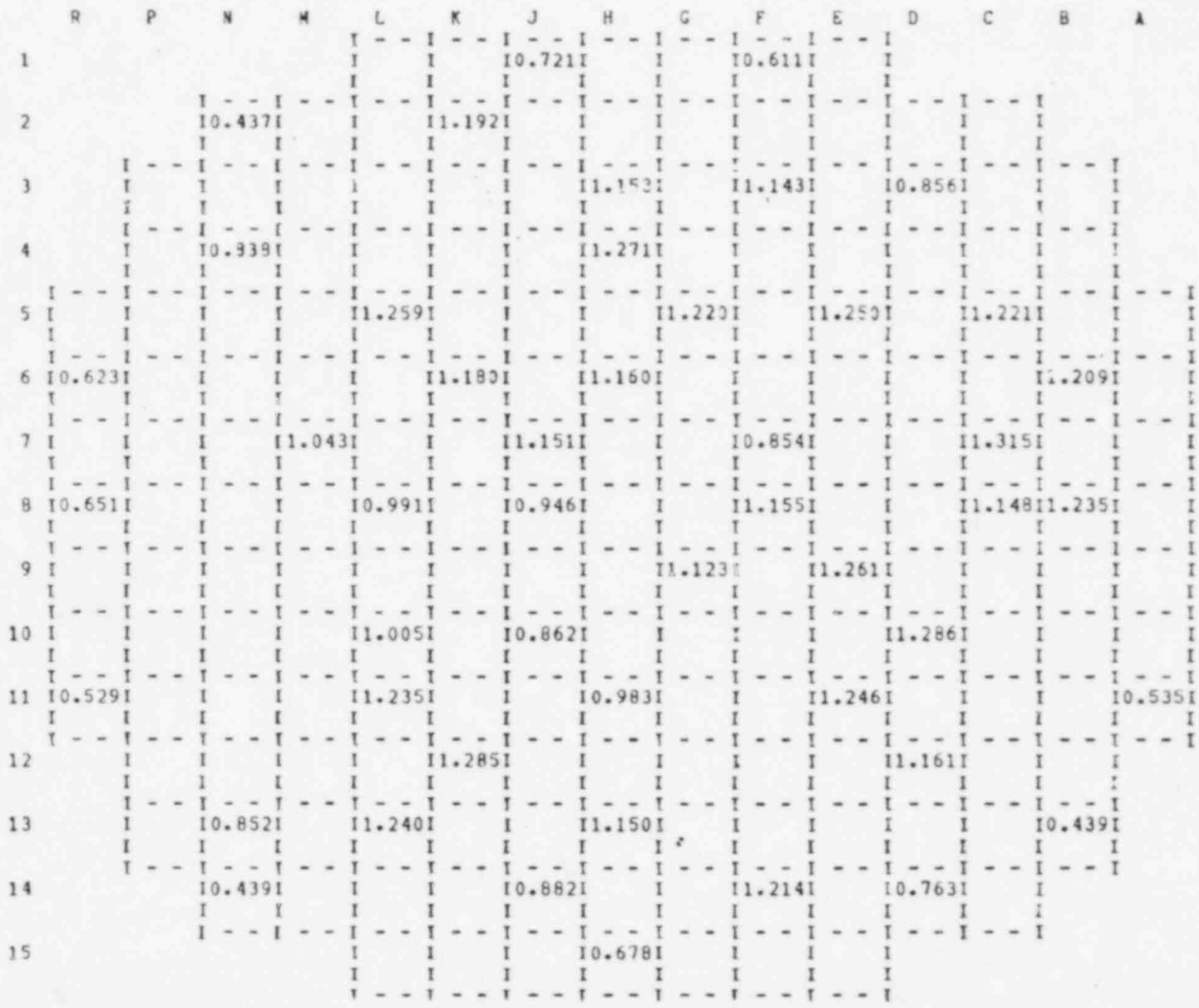

Fig. 3.7 Radially Averaged Detector Response Distribution

INFERRED FDHN FLUX MAP 2-1- 6 2-19-74

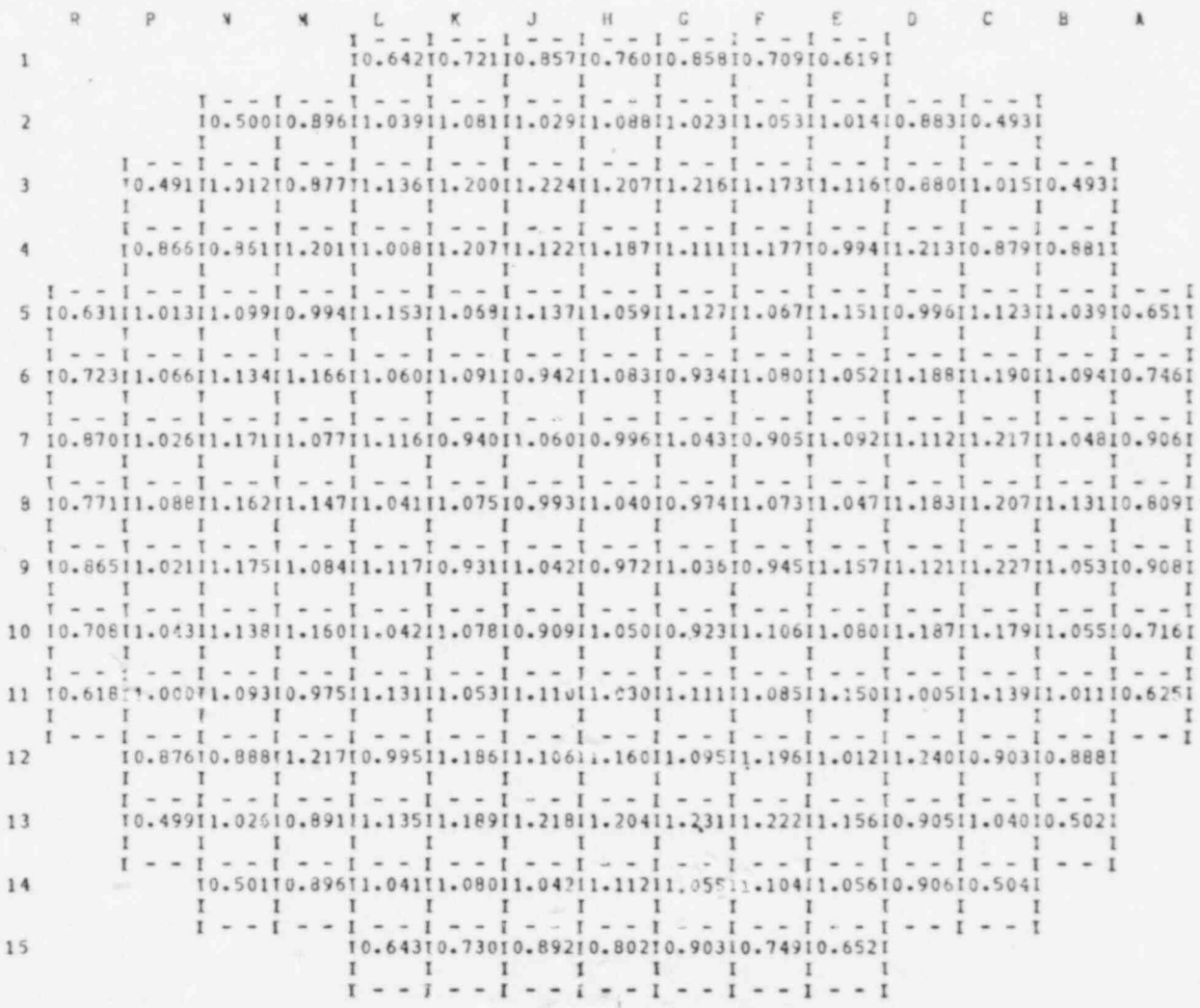

Fig. 3.8 Radial Power Distribution

AVERAGE AXIAL CONDITIONS — FLUX MAP 2-1- 6 — 2-19-74
POWER LEVEL EDITED AT 3250.0 MEGAWATTS THERMAL — AVERAGE KW/FT = 6.700

POINT	KW/FT	POINT	KW/FT
1	1.008	32	9.556
2	1.350	33	9.581
3	1.794	34	9.565
4	2.234	35	9.498
5	2.639	36	9.384
6	2.848	37	9.223
7	3.515	38	8.821
8	4.124	39	8.142
9	4.656	40	8.750
10	5.183	41	8.841
11	5.650	42	8.794
12	6.072	43	8.701
13	6.424	44	8.556
14	6.740	45	8.353
15	6.995	46	8.090
16	7.125	47	7.766
17	6.825	48	7.389
18	7.610	49	6.754
19	8.103	50	6.085
20	8.407	51	6.216
21	8.649	52	5.940
22	8.841	53	5.359
23	8.980	54	5.134
24	9.073	55	4.641
25	9.119	56	4.103
26	9.115	57	3.509
27	8.921	58	2.864
28	8.315	59	2.154
29	9.071	60	1.581
30	9.360	61	1.433
31	9.477		

FRACTION OF AVERAGE AXIAL POWER PRODUCED IN EACH REGION

REGION NO.	TOP	BOTTOM	REGION KW/FT	FRACTION OF POWER	
1	1	10	2.917	0.0653	(RODDED)
2	10	61	7.357	0.9347	(UNRODDED)

Fig. 3.9 Core Average Axial Power Distribution

The CASMO runs have included the following specific features:

a. Thermal expansion of input cold dimensions
b. Homogenization of various regions of different pins (fuel-air gap, BPR inner hole-steel tube-gap, etc.)
c. Default group energy structure
d. B1- Approximation to include leakage

Table 3.3 lists the state points for which cross section data were generated. The number of exposure and branch calculations were mainly determined by the requirements of the nodal code NODE-P and the data fitting code, SUPERLINK-P. Figures 3.10 through 3.12 show the k_∞ vs. Exposure curves as calculated by CASMO for each type of assembly.

In its present form, CASMO cannot be interfaced with any of the existing PWR ARMP modules. Therefore, certain modifications have been made in the code so that (a) one-group flux-weighted macroscopic cross sections may be calculated in accordance with the Westcott formulation [6] and (b) data generated by CASMO may be transfered to SUPERLINK-P and NODE-P.

3.3 Core Model- "B" Constants, Normalization and Albedos

Assembly data are input in NODE-P in the form of "B" constants. These constants provide detailed design data including thermal hydraulic data and values of nuclear parameters obtained as a function of various conditions such as exposure, temperature, boron concentration and control rods. Internodal leakage factors and albedos are also represented as additional input data. The "B" constants are derived by using data from a series of CASMO calculations at beginning of life (BOL), and throughout depletion (DPL). The basic one-group data transferred from CASMO to SUPERLINK-P are $\nu\Sigma_f$, $k\Sigma_f$, k_∞, M^2, N_{Xe}, and σ_{Xe}. The function of the ARMP code module, SUPERLINK-P[8] is to generate the appropriate "B" constants from the one-group quantities for a specific assembly type for use directly by NODE-P. Appendix B lists the "B" constants for all of the fuel types and describes the specific features contained in them.

The input data required for the three-dimensional nodal code, NODE-P, are the "B" constants, power level, geometric dimensions, core assembly layout, vertical and horizontal leakage factors, k_∞ multipliers, albedos, convergence criteria and thermal-hydraulic parameters. The leakage factors (g_v, g_h), k_∞ multipliers and albedos are reactor dependent and require adjustment to match BOL (or near BOL) NODE-P calculations with measured data. Once this normalization is made all these adjusting factors remain constant throughout the cycle. The NODE-P geometric representation used in this study consisted of full core, 12 axial mesh points, and a cell width of 21.4 cm. The selection

TABLE 3.3

Zion Unit-2
CASMO State Points

MOD Temp °K	Boron Concentr. ppm	Coeff.	Exposure in MWD/kg U														
			0	.5	1	2	3	5	7.5	10	12.5	15	20	25	30	35	40
535	0/1400	-	x														
535	0/1400	Control	x														
535	700	-	x												x		
560	700	Eq. Xenon	x	x	x	x	x	x	x	x	x	x	x	x	x	x	x
560	0	Eq. Xenon		x				x		x			x				
560	0	-	x	x	x	x	x			x			x		x		
560	1400	-	x														
560	700		x										x				
560	0/700/1400	Control	x														
560	700	Control and Eq. Xenon	x									x			x		
560	1400	Doppler	x														
600	0/1400	-	x														
600	0/1400	Control	x														
600	700	-	x												x		

Notes:

1. Controlled cases for type 1 and 5 fuels only
2. Some of the branch points were used for hand calculations (not input to SUPERLINK-P)

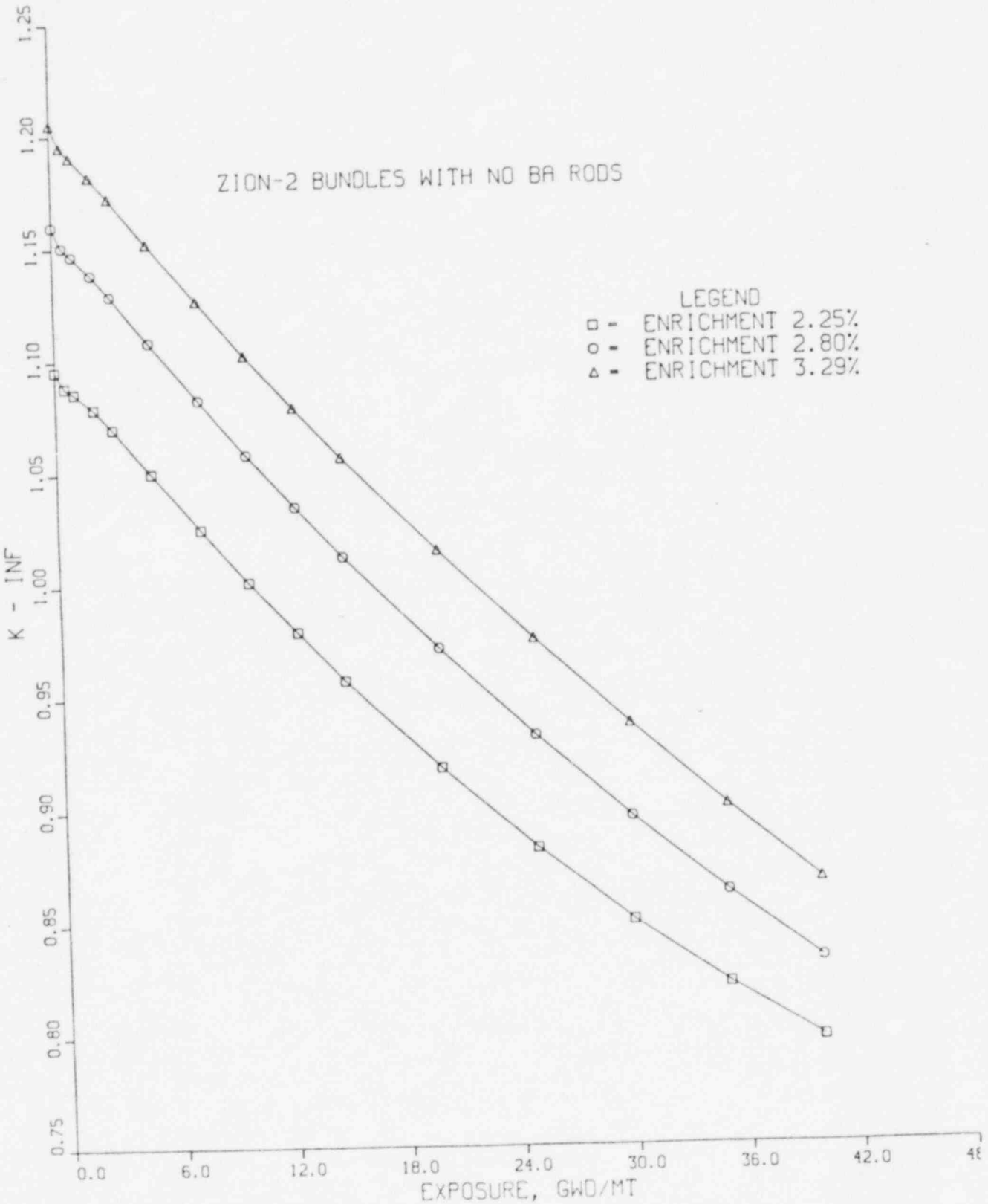

Fig. 3.10 Zion 2 Fuel Without Burnable Absorber Rods k_∞ vs. Exposure

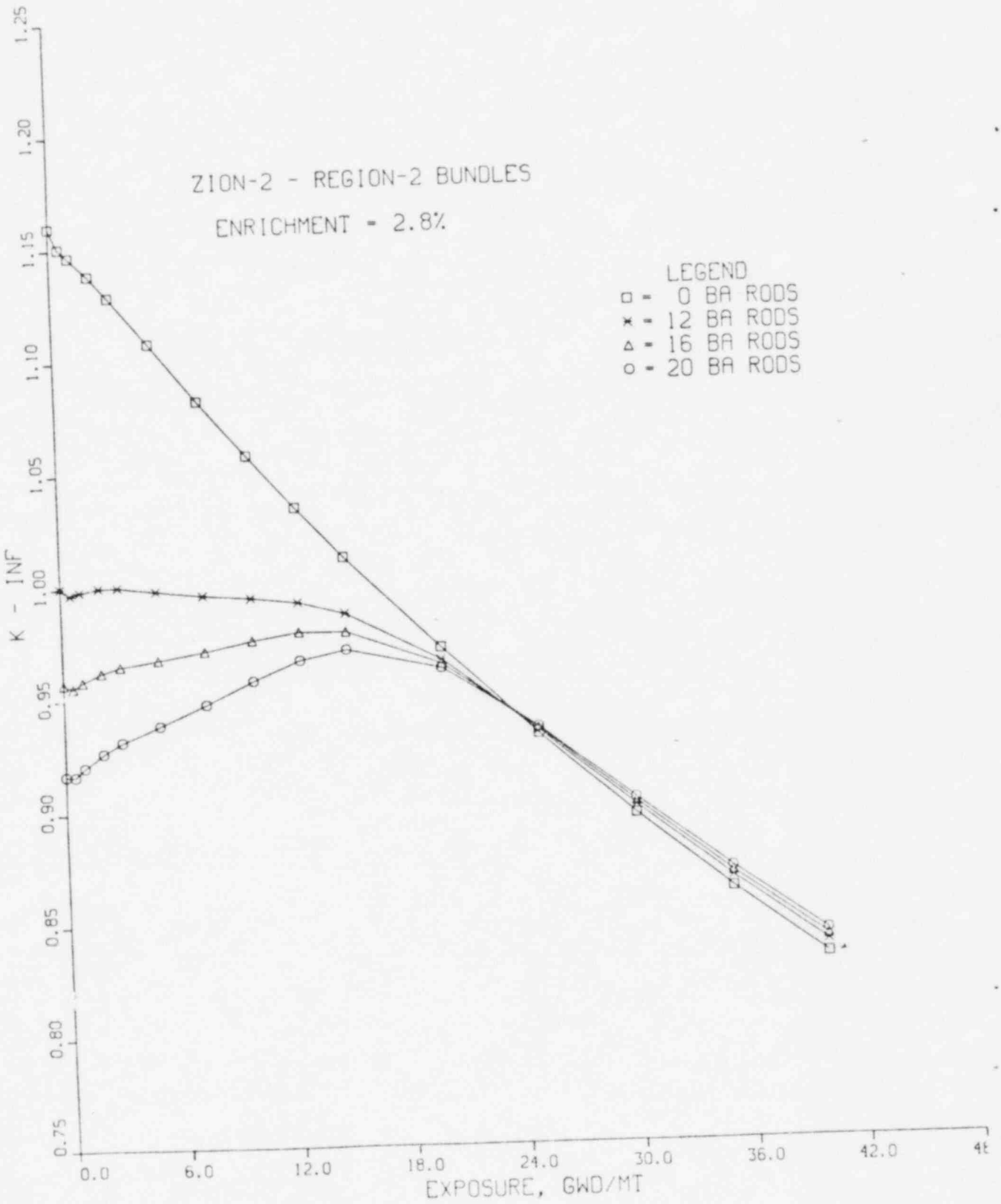

Fig. 3.11 Zion 2 Region 2 Fuel - k_∞ vs. Exposure

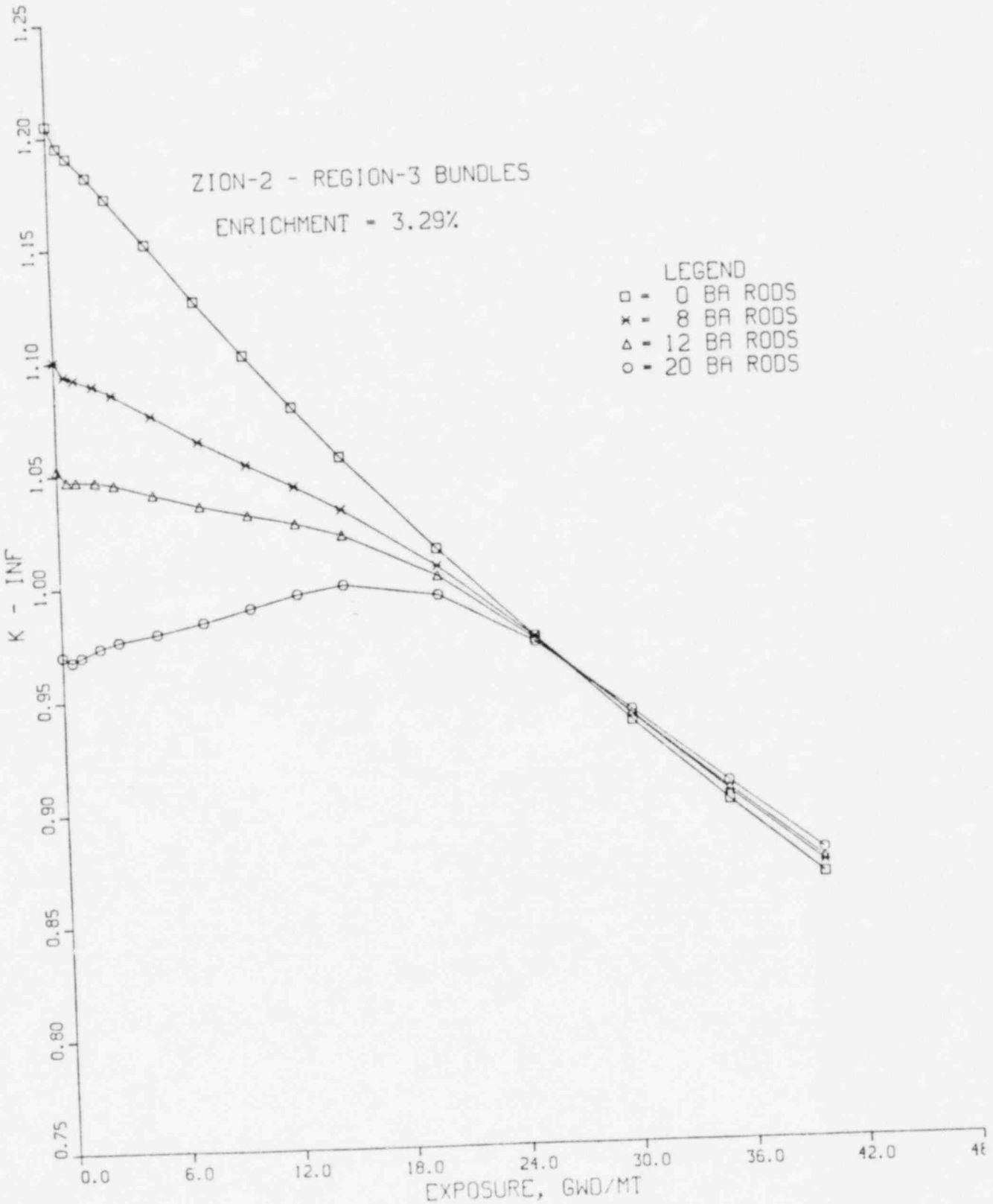

Fig. 3.12 Zion 2 Region 3 Fuel - k_∞ vs. Exposure

of the optimum set of leakage factors and albedos required an extensive series of calculations. The deviation between BOL calculations and measurements was minimized with a preliminary set of normalization factors. Since the reactor core power level was relatively low through the first 5 state points, the final selection of these parameters was made at state point 6 with 80% power. The optimum set was chosen so that the calculation/ measurement root-mean-square (RMS) errors of the radial detector reponses and the core average axial power distributions were minimized. In order to correct for interasssembly power sharing discrepancies, the assembly M^2 values may also be adjusted. This is required in the present application since unlike the 4-bundle PDQ calculations, the CASMO calculations are limited to single assembly representations and cannot properly account for interassembly coupling when the neighboring assemblies are different. For checkerboard core loadings, such as Zion Unit 2 (see Fig. 3.5), this limitation may lead to significant errors in assembly power sharing between poisoned and unpoisoned assemblies. The power in fuel assemblies containing BPR's was found to be underpredicted by $\sim 8\%$. Decreasing M^2 by 7% for type 2 and 5% for types 3 and 6 and increasing M^2 by 7% for type 1 assemblies reduced the power sharing discrepancies to a few percent.

The calculated critical boron was adjusted to match measurement by applying k_∞ multipliers. A relatively large (1.014) k_∞ adjustment factor was required to obtain good agreement. It is known that CPM underpredicts the required PDQ/NODE-P k_∞ by 0.7-0.9% at high boron concentrations.[9] Since CASMO produces almost identical results as CPM[10], it is believed that of the 1.4% adjustment in k_∞, about 0.7% can be attributed to the above mentioned effect. This slight discrepancy will be further discussed in Chapter 4.

3.4. Thermal-hydraulics

The reactor core coolant flow distribution was calculated by using THERM-P with an initial guess for the power distribution. An iteration was performed using an improved power distribution calculated by NODE-P. It was found that the relative flow distribution has converged rather rapidly and did not significantly change with varying power level. Therefore, the calculated flow distribution at BOL was considered adequate and was not changed during the cycle simulation.

4.0. RESULTS AND MEASUREMENT COMPARISONS

A description of the codes used in this evaluation is presented in chapters 2 and 3. Table 4.1 lists the exposure intervals during which operating data were collected. The principal parameters including power, exposure, neutron multiplication and temperatures have been calculated at every exposure level (state point) in each of the nodes comprising the Zion Unit 2 core. The most important results of this work, the core average radial and axial power distributions and the boron let-down curve (core eigenvalue) are discussed in the following sections.

4.1 Boron Let-Down And Start-up Measurements

The soluble boron concentration as a function of burnup for Cycle-1 is also reported with the Zion-2 measured data.[4] The tracking of the measured boron concentration is an important test of the methods used in these calculations. Figure 4.1 presents the comparison of measured and predicted boron concentrations versus core average exposure. The general agreement is reasonably good with the end-of-life accurately predicted. The core reactivity is initially somewhat underestimated, but as the core average exposure increases this discrepancy diminishes. The behavior of the boron let-down curve can be qualitatively understood in terms of the following factors.

a. BPR worth - The BOL calculations have indicated (see below) that the core model overpredicts BPR worth by ~1%. As a consequence the soluble boron requirements are underestimated in the early life of the core.

b. Assembly k_∞ - There is also some indication [9] that the CASMO assembly k_∞ values are slightly lower (.3 -.7%) than the corresponding PDQ/NODE-P values and the deviation is dependent on the amount of soluble boron present. This effect tends to reduce the core reactivity.

It should also be noted that the ARMP procedure recommends[11] an increase in the Xenon microscopic cross section by ~50% ("g"-factor) in order to produce Xe worths comparable to CPM. However, since the Zion-2 calculations were based on CASMO (which is almost identical to CPM), the Xe absorption rates were not adjusted.

TABLE 4.1 Operating State Points

Flux Map	Date	Core Burnup (MWD/MTU)	Power Level (% of 3250 MW^{th})	Bank D Position (steps withdrawn)	State Points
CYCLE 1					
2-1-6	2/19/74	53	25	191	1
2-1-7	2/25/74	128	35	181	2
2-1-9	3/18/74	273	50	208	3
2-1-26	9/21/74	753	48	203	4
2-1-27	10/07/74	1036	73	210	5
2-1-29	11/14/74	1602	82	200	6
2-1-31	3/01/75	3363	83	188	7
2-1-32	4/19/75	4229	85	193	8
2-1-33	5/22/75	5253	85	193	9
2-1-34	7/18/75	6242	85	191	10
2-1-35	8/22/75	7269	85	193	11
2-1-37	10/18/75	8188	81	196	12
2-1-38	11/18/75	9099	84	199	13
2-1-42	11/24/75	9246	84	195	14
2-1-47	1/09/76	10376	74	196	15
2-1-48	3/04/76	11132	84	218	16
2-1-51	3/23/76	11736	94	220	17
2-1-53	6/16/76	12814	94	212	18
2-1-60	7/19/76	13856	98	214	19
2-1-61	8/19/76	14785	96	220	20
2-1-62	11/04/76	15831	92	212	21
2-1-63	12/07/76	16989	97	219	22
2-1-65	1/04/77	17784	73	219	23

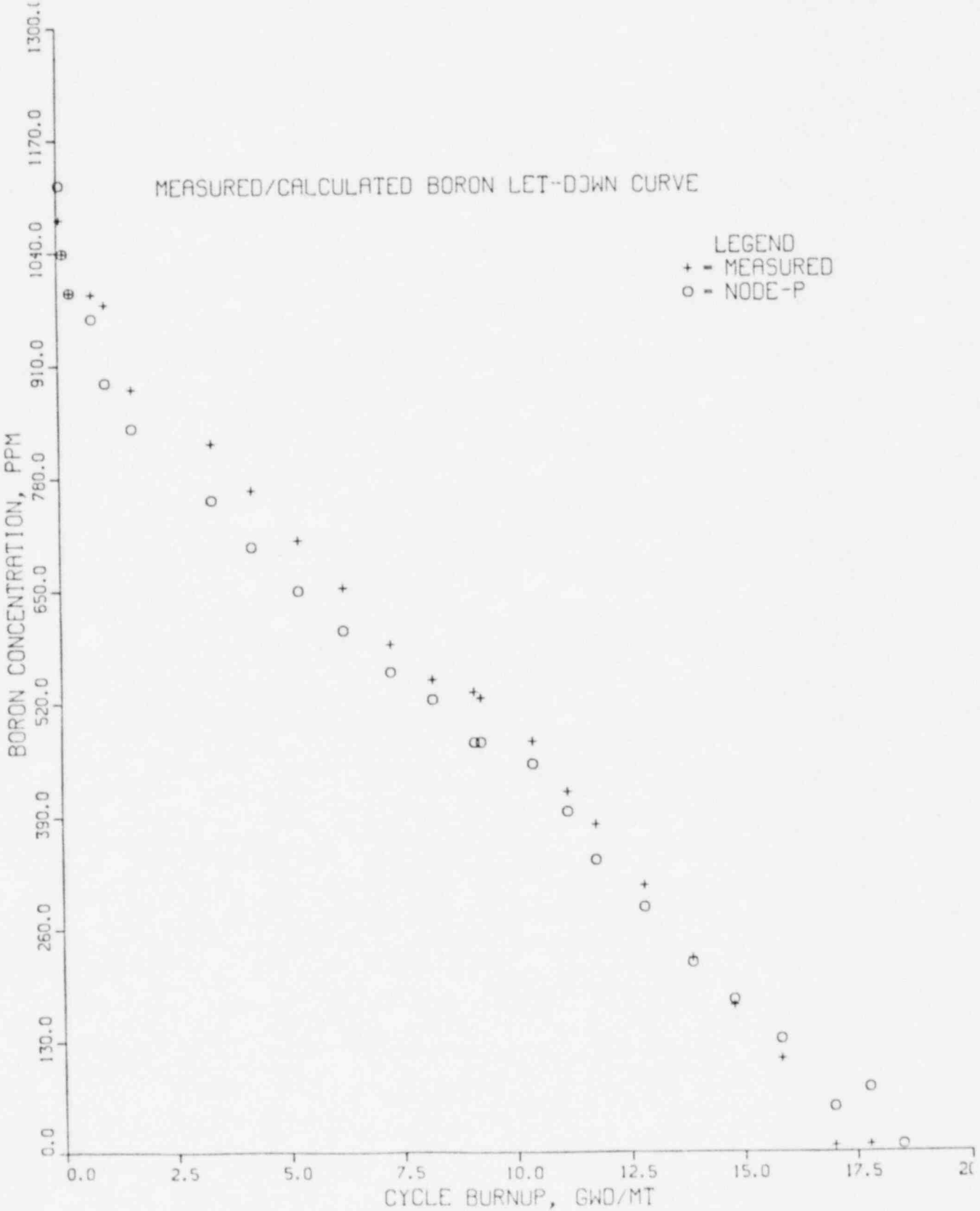

Fig. 4.1 Boron Let-Down Curve

In order to determine the validity of the NODE-P model various selected reactor physics parameters were calculated. A comparison between these parameters and similar FSAR values[12] is presented in Table 4.2. The agreement is reasonable with the BPR worth slightly overpredicted (~1%). This BPR worth overprediction is believed to be associated with the M^2 adjustment required to match the measured power sharing in assemblies containing BPR's. As a further test of the present methods various start-up measurements[4] have been simulated and in Table 4.3 and Fig. 4.2 through 4.4. the results are presented. All the measurements were done at BOL, hot zero power (HZP) conditions except for the Doppler-only power coefficients, which were done at 231 MWd/MT. The overprediction of the differential control rod worth at the top of the core can in part be attributed to the localized effect of the spacers which were neglected in the NODE-P model. The maximum differential rod worth as well as the integral worth is underpredicted. The underestimation of the control rod worth can also be seen in Table 4.3 and Fig. 4.3, where the critical boron concentrations for various control rod bank endpoints are indicated. The Doppler-only component of the differential power coefficient is accurately predicted as shown on Fig 4.4.

4.2 Power Distributions

In any nodal simulation of core behavior the calculated relative radial and axial power distributions constitute the most important elements used in assessing the success of the code to simulate the observed conditions.

Table 4.4 lists the core average RMS deviations of the calculated and measured detector, radial and axial power distributions. The detector RMS values are based on the number of detectors present in the core. The number of detectors varied from one state point to the next, averaging 40. The detector signals are direct measurements of the relative flux distribution in each axial region of the core. The calculated detector value is derived from the NODE-P power distribution using the detector-power correlation developed from data generated by CASMO. The approximations necessarily made in developing this correlation (model of the detector, no multi-bundle calculations) are such that the results are less reliable than the power predictions.

TABLE 4.2 Comparison of FSAR & Calculated

(NODE-P) Values of Selected Parameters

	FSAR	Calculated NODE-P
K_{eff}		
HZP, NoXe, B= 0 ppm	1.154	1.164
HFP, NoXe, B=0 ppm	1.132	1.140
HFP, Eq. Xe, B= 0 ppm	1.092	1.105
Boron Requirement (K_{eff}=1.0)		
HFP, No Xe	1168 ppm	1189 ppm
HFP, Eq. Xe	880 ppm	899 ppm
Coefficients		
Moderator Temp. Coeff., (pcm/°F) (HFP, B = 0, T_M = 548.6°F)	$-2.1.10^{-4}$	$-2.3.10^{-4}$
Doppler-Only Diff. Power Coeff. (pcm/%P) (P = 95% B=0, T_M = 548.6°F)	$-8.4.10^{-4}$	$-10.0.10^{-4}$
BPR Worth, % (HFP, No XE, B= 0)	9.0	10.2

Legend

HZP - Hot Zero Power
HFP - Hot Full Power
B - Boron
No Xe - No Xenon
Eq. Xe - Equilibrium Xenon
T_M - Moderator Temperature
BPR - Burnable Poison Rods

TABLE 4.3

CRITICAL BORON CONCENTRATION

Endpoint Configuration	Measured	Calculational
All Banks Withdrawn	1350	1365
Control Bank D Inserted	1209	1251
Control Banks D & C Inserted	1087	1158
Control Banks D, C & B Inserted	943	1040
Control Banks D, C, B & A Inserted	903	1006

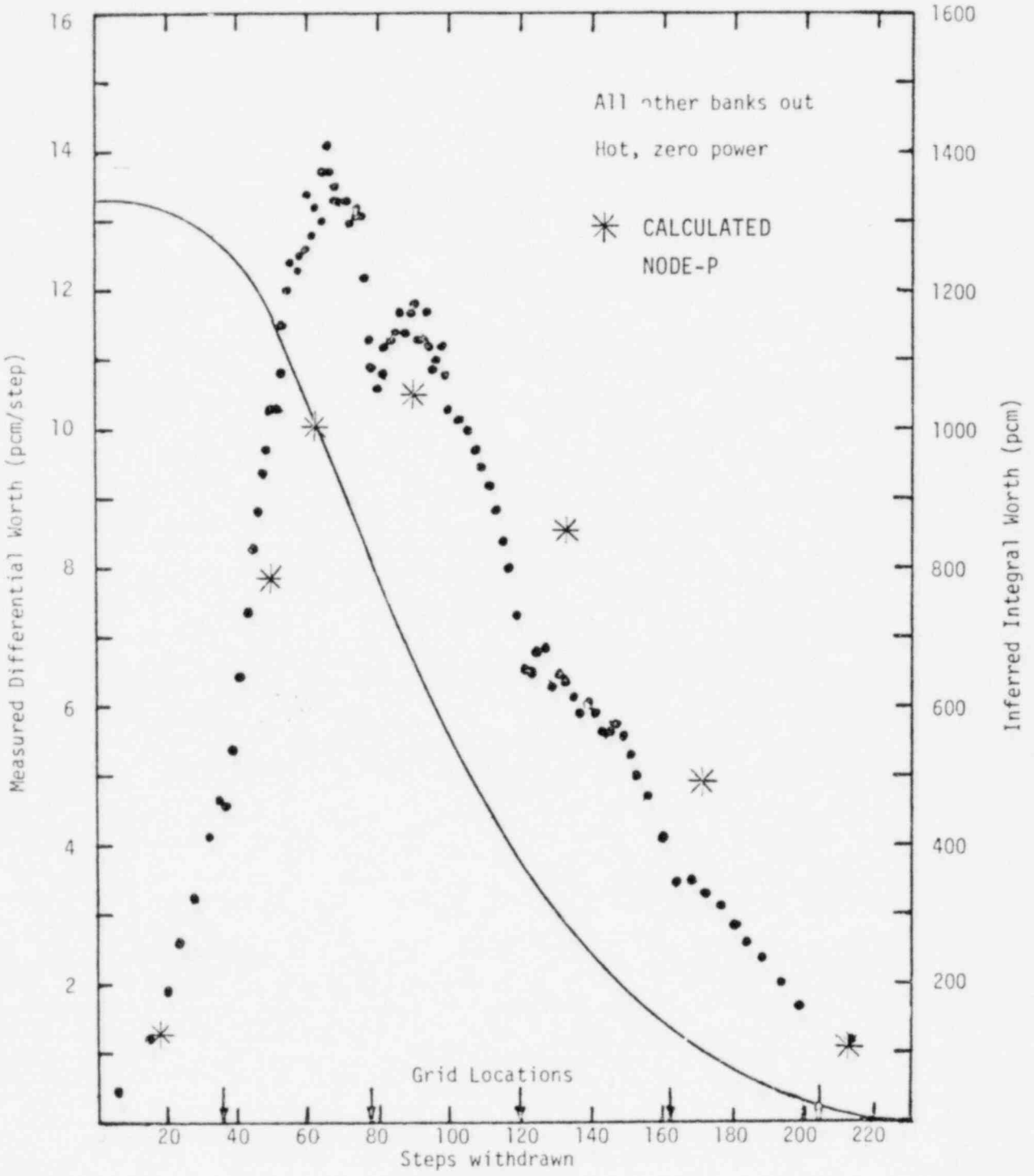

Fig. 4.2 Differential and Integral Worths of Control Bank D at Startup of Zion Unit 2, Cycle 1

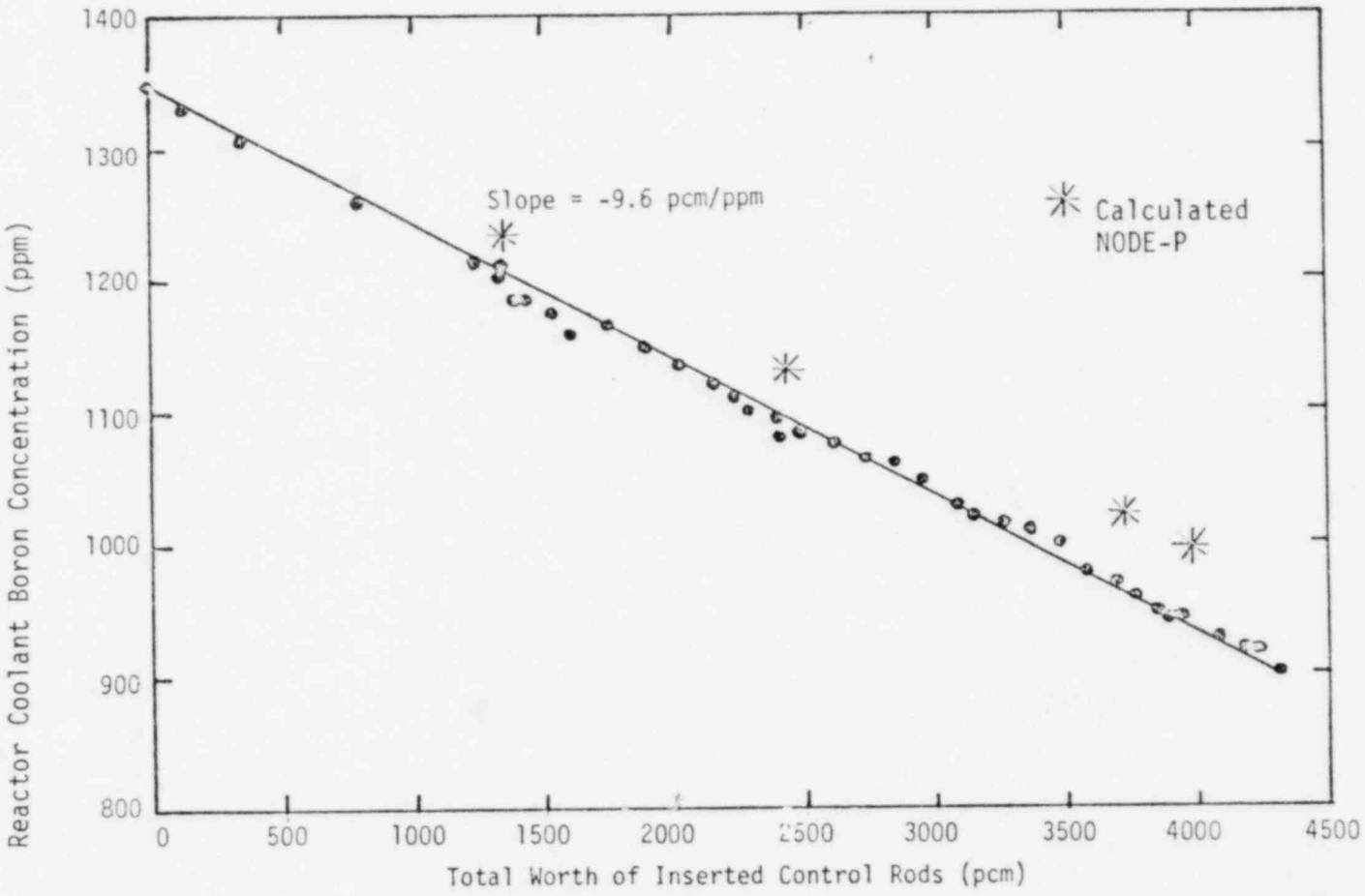

Figure 4.3 Correlation of Reactor Coolant Boron Concentration with Total Worth of Inserted Control Rods at Startup of Zion Unit 2, Cycle 1

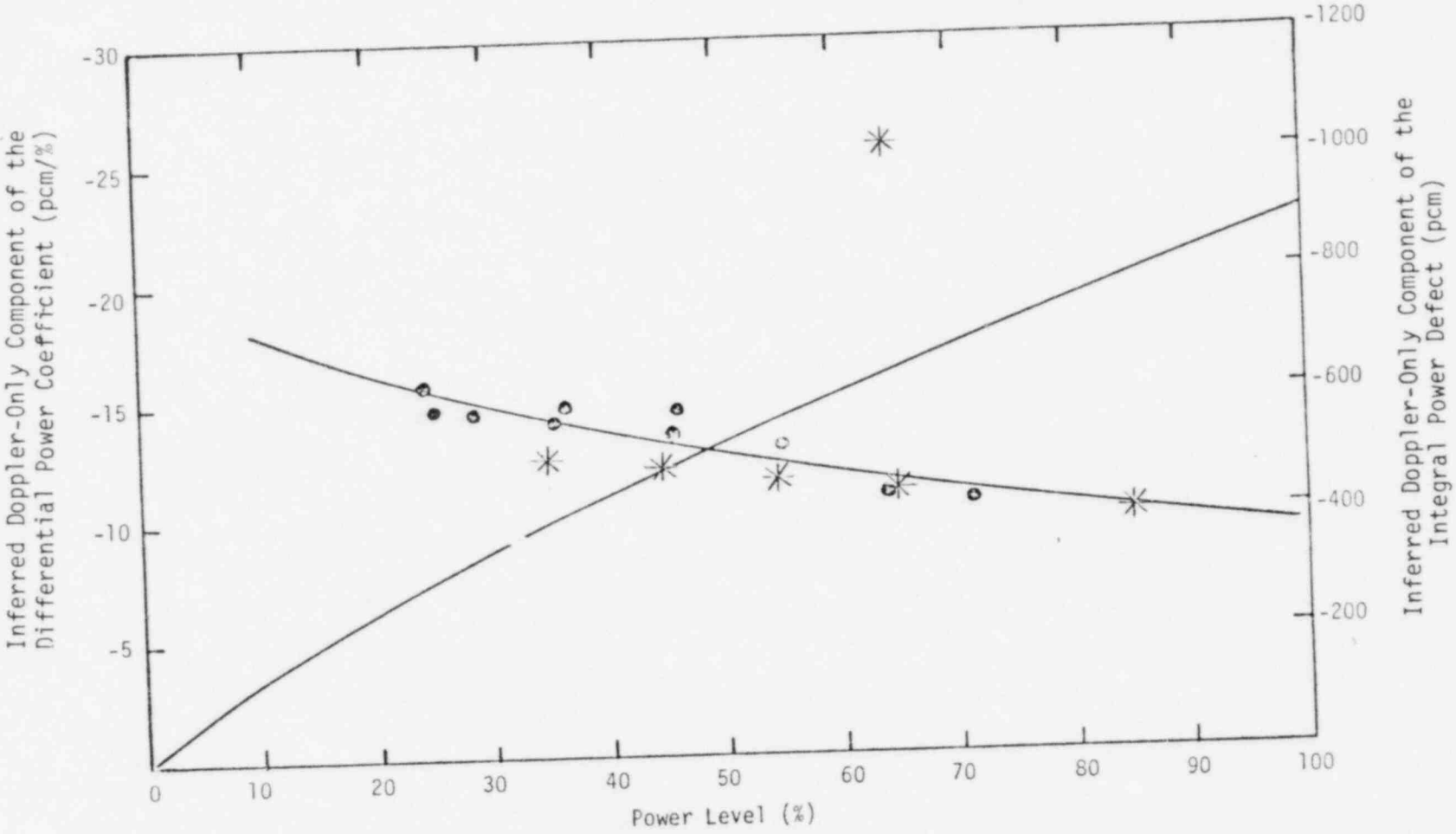

Figure 4.4 Doppler-Only Components of the Differential Power Coefficient and Integral Power Defect at Startup of Zion Unit 2, Cycle 1

TABLE 4.4 Zion Unit 2
Predicted Boron Values And Core Average Power RMS Deviations
(At Selected Points)

State Point	Exposure GWD/MT	Calc./Meas. Boron PPM	Detectors %	RMS Core Average Power Radial %	RMS Core Average Power Axial %
1	53	1117/1078	4.5	3.6	1.8
3	273	994/994	4.2	2.6	4.5
6	1602	836/882	4.6	2.8	3.1
7	3363	754/819	4.0	2.8	3.5
9	5253	649/707	3.9	2.3	3.3
11	7269	555/587	3.4	2.5	6.7
13	9099	474/531	3.7	2.2	6.0
16	11132	393/416	4.3	2.5	8.0
18	12814	283/308	4.6	2.9	5.5
20	14785	177/169	4.5	3.2	8.1
22	16989	52/7	5.8	4.2	7.1

Figures 4.5 through 4.12 show representative radial power distributions along with the percent differences (Diff% = (1-C/M) * 100) at BOL (BOL-STPT 1), middle-of-cycle (MOC-STPT 6 and 13), and end-of-cycle (EOC-STPT 23).

The BOL power level was 25% of rated, which makes the prediction of bundle powers rather difficult, since the fuel assemblies were analyzed at 100% power. Therefore, the agreement with measurement is deemed acceptable (see Fig. 4.6). There is a slight tendency to underpredict the assembly powers.

The MOC results, at STPT, 6 & 13 show better agreement (Figures 4.8 and 4.10) with core average RMS's of 2.8% and 2.2% respectively. There are no clearly detectable tendencies except that the largest difference occured in assemblies on or near the periphery of the core (Max. 7.7% and 5.8%).

The EOC power distribution shows (see Fig. 4.12) an overprediction of assembly powers in general and underprediction on the periphery. The relatively large deviations (max. 11.6%) on the periphery indicate that the BOL albedos are not fully compatible with EOC conditions. Fig. 4.13 through 4.20 show the detector responses with the percent differences at the same state points. The general behavior is the same as the above described core average radial distributions.

Fig. 4.21 through 4.24 show the core average axial distributions. There is generally very good agreement between measured and calculated values.

5.0 CONCLUSIONS

It may be stated in general that the CASMO/NODE-P code system adequately predicts the operation of Zion-2 throughout Cycle-1. The results indicate that the soluble boron concentration is underestimated in the early life of the cycle, but EOC is correctly calculated. Comparisons of measured and predicted core average radial and axial power distributions as well as detector responses indicated good agreement.

References

1. J. W. Herczeg, J. Lai, M. Todosow, and D. J. Diamond, "Simulation of A PWR First Cycle With the ARMP System," BNL-NUREG-25607, January, 1979.

2. D. Cokinos, P. Kohut, J. Lai, D. Diamond, "Simulation of Quad Cities 1 Cycle 1," BNL-NUREG-29019, June 1980.

3. P. Kohut, D. Cokinos, J. Carew, "Simulation of Ouad Cities 1 Cycle-2," BNL-NUREG-29639, May 1981.

4. A. J. Impink, Jr., B. A. Guthrie III, "Reactor Core Physics Design and Operating Data for Cycle 1 and 2 of the Zion Unit PWR Power Plant," EPRI-NP-1232, December, 1979.

5. A. Ahlin, M. Edenius, H. Haggblom, "CASMO, A Fuel Assembly Burnup Program - User's Manual," AE-RF-76-4158, June, 1978.

6. "EPRI-NODE-P," ARMP System Documentation, Part II. 4, Chapter 14, Electric Power Research Institute, 1977.

7. "EPRI-THERM--P," ARMP System Documentation, Part II. 4, Chapter 16, Electric Power Research Institute, 1977.

8. "EPRI-SUPERLINK-P," ARMP System Documentation, Part II. 4, Chapter 12, Electric Power Research Institute, 1977.

9. P. Kohut and D. Cokinos, "CASMO-CPM Comparisons," Internal Memorandum , BNL, August, 1980.

10. "EPRI-EPRI-CELL/CPM NORMALIZATION" ARMP System Documentation, Part I, Chapter 4, Electric Power Research Institute, 1977.

11. Zion Station - Final Safety Analysis Report, Volume I, Commonwealth Edison Company.

Fig. 4.5 Measured/Calculated Radial Power Distribution

Exposure 0.053GWD/MT
Boron 1117.4 ppm

				0.642 0.628	0.721 0.721	0.857 0.860	0.760 0.785	0.858 0.860	0.709 0.721	0.619 0.628				
		0.500 0.546	0.896 0.930	1.039 1.057	1.081 1.105	1.029 1.024	1.088 1.117	1.023 1.024	1.053 1.105	1.014 1.057	0.883 0.930	0.493 0.546		
	0.491 0.546	1.012 1.139	0.877 0.930	1.136 1.141	1.200 1.146	1.224 1.228	1.207 1.171	1.216 1.228	1.173 1.146	1.116 1.141	0.880 0.930	1.015 1.139	0.493 0.546	
	0.866 0.930	0.861 0.930	1.201 1.259	1.008 0.988	1.207 1.168	1.122 1.077	1.187 1.171	1.111 1.077	1.177 1.168	0.994 0.988	1.213 1.259	0.879 0.930	0.881 0.930	
0.631 0.628	1.013 1.057	1.099 1.141	0.994 0.988	1.153 1.103	1.068 1.024	1.137 1.107	1.059 1.021	1.127 1.107	1.067 1.024	1.151 1.103	0.996 0.988	1.123 1.141	1.039 1.057	0.651 0.628
0.723 0.721	1.066 1.105	1.134 1.146	1.166 1.168	1.060 1.024	1.091 1.059	0.942 0.905	1.083 1.038	0.934 0.905	1.080 1.059	1.052 1.024	1.188 1.168	1.190 1.146	1.094 1.105	0.746 0.721
0.870 0.860	1.026 1.024	1.171 1.228	1.077 1.077	1.116 1.107	0.940 0.905	1.060 1.018	0.996 0.947	1.043 1.018	0.905 0.905	1.092 1.107	1.112 1.077	1.217 1.228	1.048 1.024	0.906 0.860
0.771 0.785	1.088 1.117	1.162 1.171	1.147 1.171	1.041 1.021	1.075 1.038	0.993 0.947	1.040 1.020	0.974 0.947	1.073 1.038	1.047 1.021	1.183 1.171	1.207 1.171	1.131 1.117	0.809 0.785
0.865 0.860	1.021 1.024	1.175 1.228	1.084 1.077	1.117 1.107	0.931 0.905	1.042 1.018	0.972 0.947	1.036 1.018	0.945 0.905	1.157 1.107	1.121 1.077	1.227 1.228	1.053 1.024	0.908 0.860
0.708 0.721	1.043 1.105	1.138 1.146	1.160 1.168	1.042 1.024	1.078 1.059	0.909 0.905	1.050 1.038	0.923 0.905	1.106 1.059	1.080 1.024	1.187 1.168	1.179 1.146	1.055 1.105	0.716 0.721
0.618 0.628	1.000 1.057	1.093 1.141	0.975 0.988	1.131 1.103	1.053 1.024	1.110 1.107	1.030 1.021	1.111 1.107	1.085 1.024	1.150 1.103	1.005 0.988	1.139 1.141	1.011 1.057	0.625 0.628
	0.876 0.930	0.888 0.930	1.217 1.259	0.995 0.988	1.186 1.168	1.106 1.077	1.160 1.171	1.095 1.077	1.196 1.168	1.012 0.988	1.240 1.259	0.903 0.930	0.888 0.930	
	0.499 0.546	1.026 1.139	0.891 0.930	1.135 1.141	1.189 1.146	1.218 1.228	1.204 1.171	1.231 1.228	1.222 1.146	1.156 1.141	0.905 0.930	1.040 1.139	0.502 0.546	
		0.501 0.546	0.896 0.930	1.041 1.057	1.080 1.105	1.042 1.024	1.112 1.117	1.055 1.024	1.104 1.105	1.056 1.057	0.906 0.930	0.504 0.546		
				0.643 0.628	0.730 0.721	0.892 0.860	0.802 0.785	0.903 0.860	0.749 0.721	0.652 0.628				

1.000 ← MEASURED
1.000 ← NODE-P

Fig. 4.6 Difference In Measured/Calculated Radial Power Distribution

Exposure 0.053GWD/MT
Boron 1117.4 ppm

0.00 ← % DIFFERENCE

			2.18	0.01	-0.39	-3.34	-0.27	-1.68	-1.46				
		-9.22	-3.81	-1.73	-2.21	0.53	-2.63	-0.05	-4.93	-4.24	-5.34	-10.78	
	-11.23	-12.57	-6.01	-0.40	4.48	-0.30	3.00	-0.96	2.28	-2.20	-5.65	-12.24	-10.78
	-7.40	-7.98	-4.82	1.99	3.22	3.98	1.38	3.03	0.75	0.61	-3.78	-5.77	-5.57
0.47	-4.34	-3.78	0.61	4.36	4.14	2.65	3.60	1.78	4.05	4.20	0.81	-1.56	-1.73	3.53
0.29	-3.65	-1.08	-0.18	3.42	2.94	3.95	4.16	3.13	1.95	2.68	1.67	3.68	-1.00	3.36
1.11	0.24	-4.84	-0.03	0.82	3.75	3.94	4.93	2.37	0.03	-1.36	3.12	-0.88	2.34	5.04
-1.86	-2.63	-0.76	-2.06	1.93	3.44	4.64	1.92	2.78	3.26	2.50	1.05	3.00	1.28	2.92
0.54	-0.25	-4.49	0.62	0.90	2.82	2.28	2.58	1.71	4.26	4.33	3.90	-0.06	2.80	5.25
-1.82	-5.93	-0.72	-0.70	1.75	1.77	0.47	1.15	1.98	4.25	5.21	1.59	2.78	-4.73	-0.68
-1.62	-5.70	-4.35	-1.33	2.50	2.78	0.28	0.89	0.37	5.64	4.12	1.70	-0.14	-4.55	-0.48
	-6.18	-4.70	-3.44	0.71	1.51	2.59	-0.92	1.61	2.33	2.38	-1.52	-2.96	-4.74	
	-9.44	-11.04	-4.35	-0.49	3.60	-0.80	2.76	0.27	6.20	1.34	-2.73	-9.54	-8.79	
		-9.01	-3.81	-1.53	-2.30	1.77	-0.41	2.98	-0.08	-0.09	-2.66	-8.36	
				2.33	1.25	3.55	2.07	4.72	3.75	3.68			

Fig. 4.7 Measured/Calculated Radial Power Distribution

Exposure 1.602GWD/MT
Boron 836.0 ppm

				0.610 0.593	0.699 0.686	0.873 0.806	0.801 0.746	0.852 0.806	0.679 0.686	0.593 0.593				
		0.474 0.505	0.848 0.854	0.989 0.997	1.032 1.058	1.014 1.001	1.117 1.079	1.009 1.001	1.002 1.058	0.975 0.997	0.852 0.854	0.500 0.505		
	0.469 0.505	0.975 1.022	0.854 0.901	1.004 1.105	1.143 1.138	1.207 1.205	1.167 1.169	1.214 1.205	1.102 1.138	1.082 1.105	0.851 0.901	1.031 1.022	0.524 0.505	
	0.828 0.854	0.854 0.901	1.185 1.187	0.954 1.014	1.139 1.181	1.131 1.122	1.230 1.190	1.128 1.122	1.185 1.181	0.961 1.014	1.194 1.187	0.887 0.901	0.915 0.854	
0.591 0.593	0.975 0.997	1.082 1.105	0.964 1.014	1.100 1.136	1.061 1.093	1.189 1.167	1.102 1.102	1.163 1.167	1.075 1.093	1.138 1.136	0.991 1.014	1.111 1.105	0.994 0.997	0.598 0.593
0.678 0.686	1.022 1.058	1.160 1.138	1.172 1.181	1.068 1.093	1.134 1.136	0.996 1.013	1.129 1.132	0.977 1.013	1.125 1.136	1.082 1.093	1.186 1.181	1.159 1.138	1.020 1.058	0.685 0.686
0.843 0.806	1.010 1.001	1.220 1.205	1.135 1.122	1.173 1.167	1.008 1.013	1.146 1.124	1.068 1.067	1.120 1.124	0.984 1.013	1.193 1.167	1.146 1.122	1.222 1.205	1.023 1.001	0.855 0.806
0.770 0.746	1.095 1.079	1.221 1.169	1.212 1.190	1.093 1.102	1.172 1.132	1.087 1.067	1.154 1.127	1.067 1.067	1.160 1.132	1.105 1.102	1.232 1.190	1.232 1.169	1.105 1.079	0.765 0.746
0.864 0.806	1.021 1.001	1.217 1.205	1.126 1.122	1.152 1.167	1.000 1.013	1.147 1.124	1.077 1.067	1.159 1.124	0.991 1.013	1.155 1.167	1.140 1.122	1.244 1.205	1.022 1.001	0.841 0.806
0.705 0.686	1.045 1.058	1.165 1.138	1.180 1.181	1.071 1.093	1.133 1.136	1.005 1.013	1.147 1.132	1.000 1.013	1.098 1.136	1.066 1.093	1.195 1.181	1.196 1.138	1.025 1.058	0.694 0.686
0.611 0.593	0.990 0.997	1.085 1.105	0.986 1.014	1.137 1.136	1.097 1.093	1.201 1.167	1.108 1.102	1.175 1.167	1.060 1.093	1.110 1.136	0.967 1.014	1.088 1.105	0.987 0.997	0.609 0.593
	0.860 0.854	0.866 0.901	1.200 1.187	1.001 1.014	1.234 1.181	1.144 1.122	1.192 1.190	1.123 1.122	1.175 1.181	0.947 1.014	1.142 1.187	0.842 0.901	0.867 0.854	
	0.483 0.505	0.998 1.022	0.864 0.901	1.104 1.105	1.199 1.138	1.208 1.205	1.160 1.169	1.197 1.205	1.180 1.138	1.078 1.105	0.832 0.901	0.982 1.022	0.490 0.505	
		0.483 0.505	0.863 0.854	0.999 0.997	1.042 1.058	0.995 1.001	1.061 1.079	1.011 1.001	1.065 1.058	1.000 0.997	0.844 0.854	0.479 0.505		
				0.615 0.593	0.705 0.686	0.855 0.806	0.762 0.746	0.862 0.806	0.722 0.686	0.617 0.593				

1.000 ← MEASURED
1.000 ← NODE-P

Fig. 4.8 Difference In
Measured/Calculated Radial Power Distribution

Exposure 1.602GWD/MT
Boron 836.0 ppm

0.00 ← % DIFFERENCE

			2.82	1.86	7.70	6.82	5.42	-1.03	0.04				
		-6.52	-0.71	-0.79	-2.55	1.26	3.37	0.77	-5.62	-2.23	-0.24	-0.98	
	-7.66	-4.84	-5.46	-10.03	0.46	0.13	-0.20	0.71	-3.25	-2.10	-5.83	0.85	3.64
	-3.14	-5.46	-0.14	-6.27	-3.68	0.80	3.27	0.54	0.34	-5.49	0.61	-1.54	6.66
-0.30	-2.23	-2.10	-5.16	-3.25	-3.01	1.82	0.03	-0.38	-1.67	0.20	-2.30	0.57	-0.28	0.87
-1.18	-3.55	1.91	-0.76	-2.34	-0.21	-1.75	-0.30	-3.73	-1.01	-1.02	0.43	1.83	-3.76	-0.14
4.42	0.87	1.20	1.15	0.48	-0.54	1.92	0.11	-0.36	-2.99	2.15	2.10	1.36	2.13	5.76
3.07	1.43	4.23	1.83	-0.80	3.38	1.86	2.34	0.02	2.38	0.30	3.43	5.09	2.32	2.43
6.74	1.94	0.95	0.36	-1.34	-1.34	2.01	0.95	3.02	-2.26	-1.07	1.59	3.10	2.04	4.19
2.70	-1.28	2.34	-0.08	-2.05	-0.30	-0.84	1.27	-1.34	-3.50	-2.53	1.18	4.87	-3.25	1.16
2.98	-0.68	-1.82	-2.92	0.11	0.37	2.80	0.57	0.65	-3.11	-2.32	-4.84	-1.54	-0.99	2.66
	0.69	-4.00	1.11	-1.28	4.30	1.93	0.19	0.10	-0.50	-7.05	-3.91	-6.97	1.49	
	-4.54	-2.42	-4.24	-0.07	5.11	0.21	-0.80	-0.70	3.58	-2.48	-8.25	-4.09	-3.04	
		-4.54	1.04	0.22	-1.57	-0.62	-1.73	0.97	0.63	0.32	-1.19	-5.41		
				3.61	2.70	5.76	2.05	6.52	4.99	3.93				

Fig. 4.9 Measured/Calculated Radial Power Distribution

Exposure 9.099GWD/MT
Boron 473.5 ppm

				0.597 0.577	0.682 0.661	0.779 0.757	0.726 0.709	0.782 0.757	0.670 0.661	0.580 0.577				
		0.509 0.509	0.838 0.828	0.975 0.980	0.967 0.969	1.001 1.011	0.994 0.985	1.004 1.011	0.957 0.969	0.969 0.980	0.843 0.828	0.505 0.509		
	0.504 0.509	0.974 0.986	0.938 0.977	1.048 1.050	1.143 1.125	1.118 1.100	1.182 1.135	1.117 1.100	1.148 1.125	1.055 1.050	0.936 0.977	0.972 0.986	0.502 0.509	
	0.833 0.828	0.935 0.977	1.167 1.143	1.089 1.114	1.147 1.129	1.189 1.168	1.136 1.107	1.165 1.168	1.123 1.129	1.070 1.114	1.157 1.143	0.930 0.977	0.836 0.828	
0.587 0.577	0.971 0.980	1.054 1.050	1.081 1.114	1.142 1.128	1.170 1.185	1.170 1.151	1.180 1.187	1.136 1.151	1.151 1.185	1.123 1.128	1.068 1.114	1.050 1.050	0.976 0.980	0.598 0.577
0.674 0.661	0.962 0.969	1.156 1.125	1.142 1.129	1.172 1.185	1.145 1.152	1.133 1.169	1.173 1.156	1.124 1.169	1.139 1.152	1.161 1.185	1.114 1.129	1.135 1.125	0.968 0.969	0.691 0.661
0.789 0.757	1.015 1.011	1.127 1.100	1.174 1.168	1.163 1.151	1.137 1.169	1.166 1.159	1.196 1.199	1.156 1.159	1.121 1.169	1.150 1.151	1.145 1.168	1.080 1.100	0.997 1.011	0.796 0.757
0.739 0.709	1.013 0.985	1.205 1.135	1.140 1.107	1.195 1.187	1.179 1.156	1.205 1.199	1.149 1.139	1.168 1.199	1.147 1.156	1.168 1.187	1.115 1.107	1.161 1.135	0.986 0.985	0.726 0.709
0.801 0.757	1.014 1.011	1.129 1.100	1.192 1.168	1.174 1.151	1.147 1.169	1.177 1.159	1.186 1.199	1.148 1.159	1.121 1.169	1.151 1.151	1.156 1.168	1.104 1.100	1.000 1.011	0.786 0.757
0.679 0.661	0.961 0.969	1.152 1.125	1.141 1.129	1.181 1.185	1.158 1.152	1.140 1.169	1.169 1.156	1.134 1.169	1.142 1.152	1.153 1.185	1.115 1.129	1.134 1.125	0.955 0.969	0.680 0.661
0.578 0.577	0.943 0.980	1.015 1.050	1.077 1.114	1.125 1.128	1.175 1.185	1.172 1.151	1.196 1.187	1.169 1.151	1.156 1.155	1.114 1.128	1.073 1.114	1.065 1.050	0.958 0.980	0.587 0.577
	0.824 0.828	0.928 0.977	1.147 1.143	1.071 1.114	1.144 1.129	1.173 1.168	1.124 1.107	1.169 1.168	1.132 1.129	1.081 1.114	1.185 1.143	0.954 0.977	0.836 0.828	
	0.504 0.509	0.970 0.986	0.926 0.977	1.042 1.050	1.153 1.125	1.110 1.100	1.160 1.135	1.109 1.100	1.159 1.125	1.061 1.050	0.941 0.977	0.981 0.986	0.508 0.509	
		0.505 0.509	0.828 0.828	0.948 0.980	0.942 0.969	1.009 1.011	0.996 0.985	1.010 1.011	0.978 0.969	0.972 0.980	0.826 0.828	0.502 0.509		
				0.570 0.577	0.659 0.661	0.800 0.757	0.739 0.709	0.801 0.757	0.697 0.661	0.596 0.577				

1.000 ← MEASURED
1.000 ← NODE-P

Fig. 4.10 Difference In
Measured/Calculated Radial Power Distribution

Exposure 9.099GWD/MT
Boron 473.5 ppm

0.00 ← % DIFFERENCE

			3.42	3.15	2.80	2.32	3.18	1.41	0.59				
		-0.07	1.14	-0.47	-0.26	-1.04	0.89	-0.74	-1.31	-1.09	1.73	-0.86	
	-1.06	-1.23	-4.12	-0.20	1.61	1.58	3.95	1.49	2.03	0.47	-4.34	-1.44	-1.46
	0.55	-4.45	2.09	-2.29	1.59	1.79	2.56	-0.23	-0.52	-4.11	1.25	-5.01	0.90
1.78	-0.89	0.37	-3.05	1.20	-1.29	1.60	-0.58	-1.34	-2.96	-0.47	-4.30	-0.01	-0.37	3.58
2.00	-0.78	2.71	1.16	-1.11	-0.63	-3.13	1.46	-3.96	-1.16	-2.07	-1.33	0.91	-0.15	4.41
4.04	0.35	2.36	0.53	1.01	-2.77	0.57	-0.21	-0.29	-4.24	-0.11	-1.98	-1.89	-1.44	4.88
4.04	2.75	5.79	2.91	0.68	1.96	0.53	0.85	-2.62	-0.77	-1.62	0.73	2.22	0.08	2.32
5.47	0.26	2.53	2.04	1.94	-1.88	1.50	-1.06	-0.99	-4.24	-0.02	-1.01	0.33	-1.14	3.67
2.72	-0.88	2.37	1.07	-0.34	0.50	-2.50	1.13	-3.04	-0.90	-2.78	-1.24	0.82	-1.52	2.86
0.25	-3.88	-3.45	-3.43	-0.29	-0.85	1.77	0.76	1.52	-2.51	-1.28	-3.82	1.40	-2.25	1.78
	-0.54	-5.24	0.38	-4.01	1.33	0.45	1.52	0.11	0.28	-3.05	3.58	-2.37	0.90	
	-1.06	-1.64	-5.47	-0.77	2.46	0.87	2.13	0.78	2.96	1.03	-3.79	-0.51	-0.26	
		-0.86	-0.05	-3.33	-2.92	-0.24	1.09	-0.14	0.87	-0.78	-0.30	-1.46		
				-1.15	-0.23	5.36	4.04	5.47	5.23	3.26				

Fig. 4.11 Measured/Calculated Radial Power Distribution

Exposure 17.784GWD/MT
Boron 74.1 ppm

1.000 ← MEASURED
1.000 ← NODE-P

			0.642 0.603	0.774 0.693	0.845 0.778	0.836 0.739	0.833 0.778	0.752 0.693	0.624 0.603					
		0.609 0.552	0.914 0.862	1.060 1.028	0.987 0.958	1.121 1.088	1.027 0.974	1.098 1.088	0.962 0.958	1.034 1.028	0.880 0.862	0.605 0.552		
	0.605 0.552	1.069 1.026	1.112 1.101	1.066 1.044	1.137 1.111	1.065 1.044	1.157 1.106	1.057 1.044	1.112 1.111	1.042 1.044	1.078 1.101	1.069 1.026	0.605 0.552	
	0.902 0.862	1.097 1.101	1.164 1.174	1.124 1.180	1.036 1.066	1.151 1.146	1.072 1.045	1.121 1.146	1.037 1.066	1.124 1.180	1.162 1.174	1.089 1.101	0.896 0.862	
0.633 0.603	1.046 1.028	1.060 1.044	1.124 1.180	1.060 1.081	1.111 1.164	1.057 1.067	1.146 1.152	1.078 1.067	1.103 1.164	1.053 1.081	1.122 1.180	1.049 1.044	1.045 1.028	0.641 0.603
0.757 0.693	0.965 0.958	1.115 1.111	1.037 1.066	1.109 1.164	1.035 1.074	1.095 1.171	1.034 1.070	1.078 1.171	1.027 1.074	1.103 1.164	1.034 1.066	1.121 1.111	0.974 0.958	0.772 0.693
0.825 0.778	1.111 1.088	1.053 1.044	1.115 1.146	1.030 1.067	1.100 1.171	1.043 1.072	1.119 1.159	1.057 1.072	1.120 1.171	1.061 1.067	1.128 1.146	1.052 1.044	1.108 1.088	0.832 0.778
0.806 0.739	1.005 0.974	1.125 1.106	1.040 1.045	1.093 1.152	1.041 1.070	1.119 1.159	1.028 1.058	1.104 1.159	1.020 1.070	1.099 1.152	1.027 1.045	1.138 1.106	1.005 0.974	0.817 0.739
0.825 0.778	1.110 1.088	1.052 1.044	1.116 1.146	1.027 1.067	1.090 1.171	1.033 1.072	1.094 1.159	1.035 1.072	1.077 1.171	1.029 1.067	1.099 1.146	1.047 1.044	1.112 1.088	0.837 0.778
0.757 0.693	0.966 0.958	1.113 1.111	1.036 1.066	1.102 1.164	1.025 1.074	1.083 1.171	1.021 1.070	1.085 1.171	1.013 1.074	1.090 1.164	1.026 1.066	1.118 1.111	0.985 0.958	0.773 0.693
0.628 0.603	1.038 1.028	1.043 1.044	1.124 1.180	1.066 1.081	1.112 1.164	1.033 1.067	1.095 1.152	1.035 1.067	1.112 1.164	1.053 1.081	1.125 1.180	1.044 1.044	1.054 1.028	0.638 0.603
	0.911 0.862	1.108 1.101	1.196 1.174	1.155 1.180	1.065 1.066	1.108 1.146	1.028 1.045	1.104 1.146	1.046 1.066	1.123 1.180	1.163 1.174	1.075 1.101	0.901 0.862	
	0.607 0.552	1.072 1.026	1.108 1.101	1.072 1.044	1.109 1.111	1.022 1.044	1.097 1.106	1.041 1.044	1.139 1.111	1.057 1.044	1.075 1.101	1.041 1.026	0.589 0.552	
		0.607 0.552	0.897 0.862	1.032 1.028	0.945 0.958	1.086 1.088	0.984 0.974	1.112 1.088	0.994 0.958	1.068 1.028	0.884 0.862	0.589 0.552		
			0.625 0.603	0.742 0.693	0.819 0.778	0.802 0.739	0.845 0.778	0.780 0.693	0.647 0.603					

Fig. 4.12 Difference In
Measured/Calculated Radial Power Distribution

Exposure 17.784GWD/MT
Boron 74.1 ppm

0.00 ← % DIFFERENCE

			6.02	10.51	7.94	11.65	6.61	7.89	3.31				
		9.29	5.68	3.00	2.91	2.93	5.20	0.90	0.39	0.56	2.04	8.69	
	8.69	4.05	0.99	2.05	2.25	2.02	4.43	1.27	0.06	-0.21	-2.14	4.05	8.69
	4.43	-0.37	-0.86	-5.02	-2.93	0.39	2.56	-2.27	-2.84	-5.02	-1.03	-1.10	3.79
4.68	1.70	1.49	-5.02	-1.99	-4.76	-0.91	0.54	1.05	-5.52	-2.66	-5.21	0.46	1.61	5.87
8.50	0.70	0.32	-2.84	-4.95	-3.78	-6.92	-3.50	-8.61	-4.59	-5.52	-3.13	0.86	1.62	10.28
5.71	2.06	0.90	-2.82	-3.56	-6.44	-2.75	-3.54	-1.39	-4.54	-0.53	-1.64	0.80	1.79	6.50
8.36	3.13	1.71	-0.44	-5.41	-2.80	-3.54	-2.90	-4.94	-4.92	-4.84	-1.71	2.83	3.13	9.60
5.71	1.97	0.80	-2.73	-3.86	-7.41	-3.74	-5.90	-3.54	-8.71	-3.66	-4.32	0.33	2.14	7.06
8.50	0.80	0.15	-2.93	-5.62	-4.79	-8.11	-4.81	-7.91	-6.03	-6.78	-3.94	0.59	2.72	10.40
3.93	0.94	-0.11	-5.02	-1.41	-4.67	-3.26	-5.22	-3.06	-4.67	-2.66	-4.93	-0.02	2.45	5.43
	5.37	0.63	1.84	-2.21	-0.13	-3.47	-1.61	-3.85	-1.95	-5.12	-0.95	-2.42	4.32	
	8.99	4.32	0.63	2.60	-0.21	-2.11	-0.80	-0.24	2.43	1.21	-2.42	1.47	6.21	
		8.99	3.89	0.37	-1.40	-0.20	1.06	2.14	3.60	3.73	2.48	6.21	
				3.46	6.65	5.01	7.91	7.94	11.20	6.75			

Fig. 4.13 Measured/Calculated Detector Response Factor

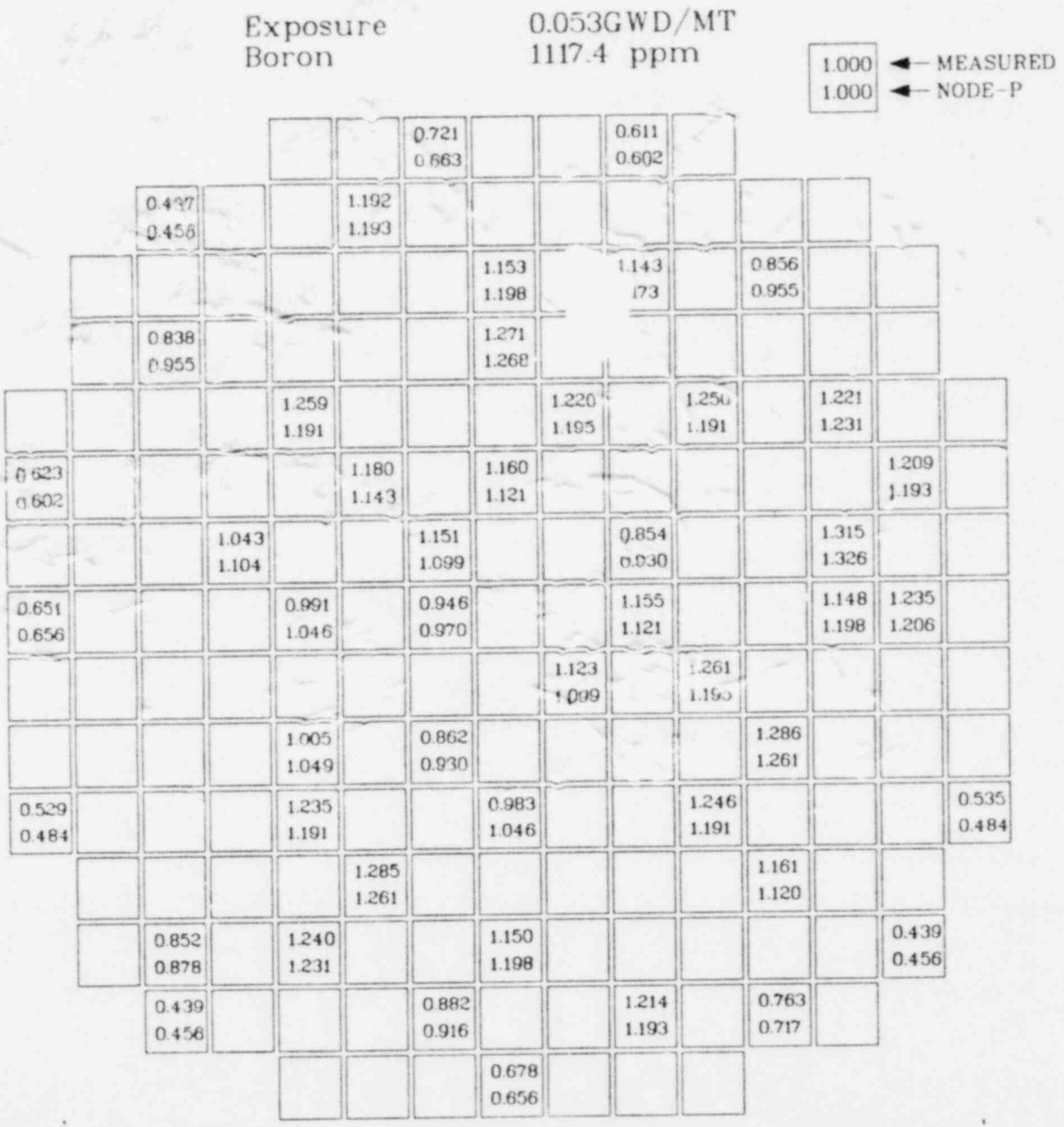

Fig. 4.14 Difference In
Measured/Calculated Detector Response Factor

Exposure 0.053GWD/MT
Boron 1117.4 ppm

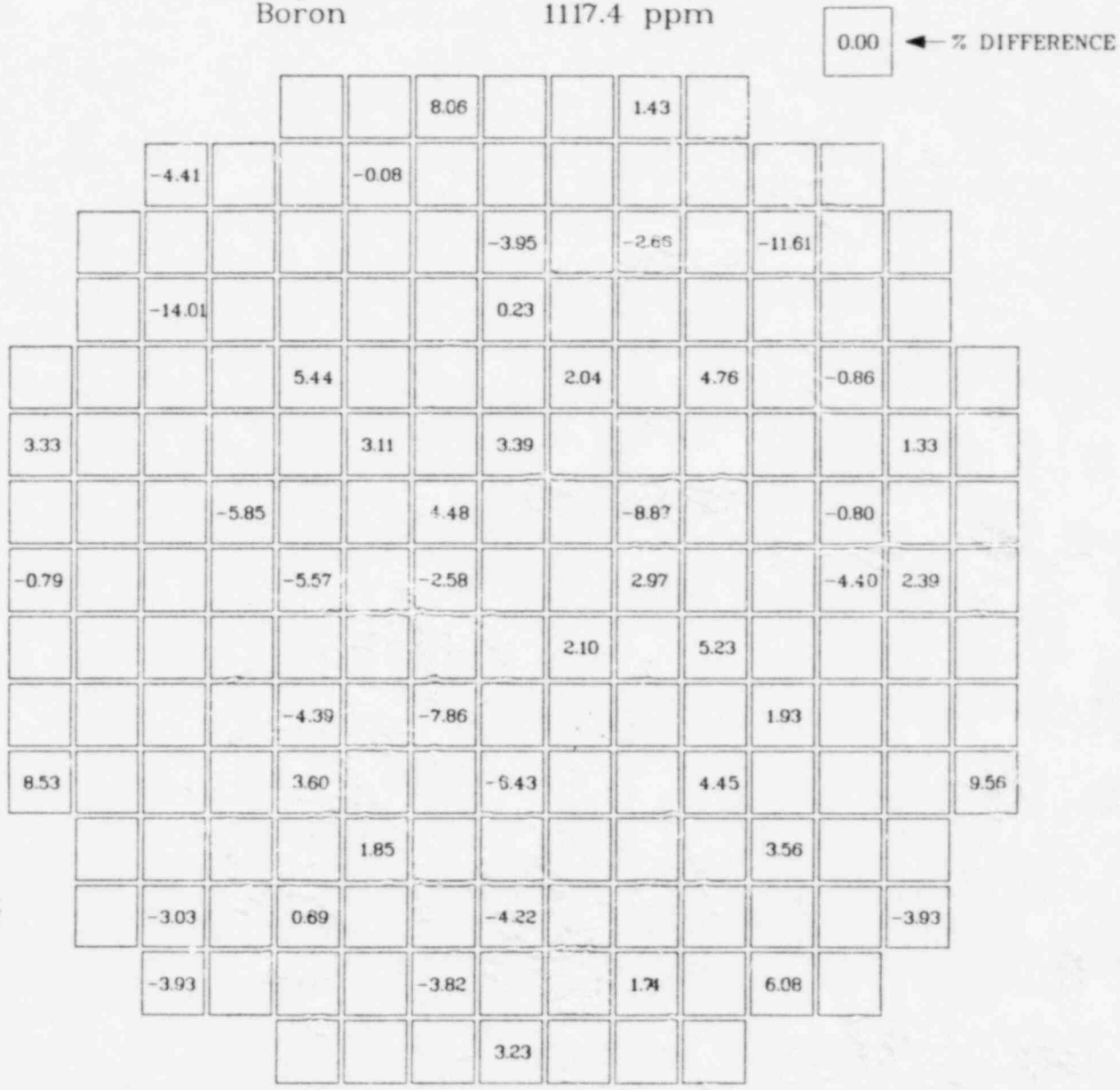

Fig. 4.15 Measured/Calculated Detector Response Factor

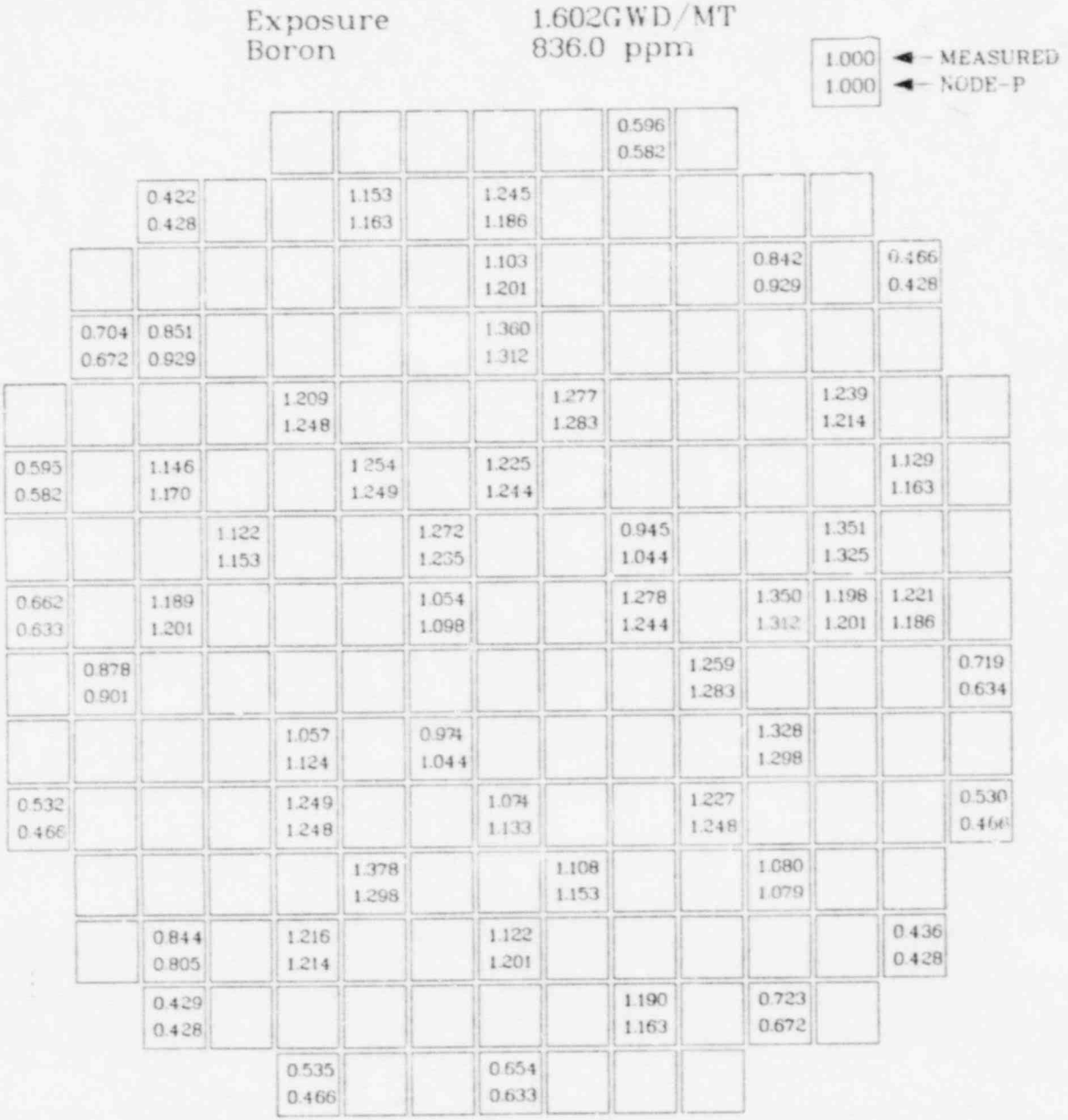

Fig 4.16 Difference In
Measured/Calculated Detector Response Factor

Exposure 1.602GWD/MT
Boron 836.0 ppm

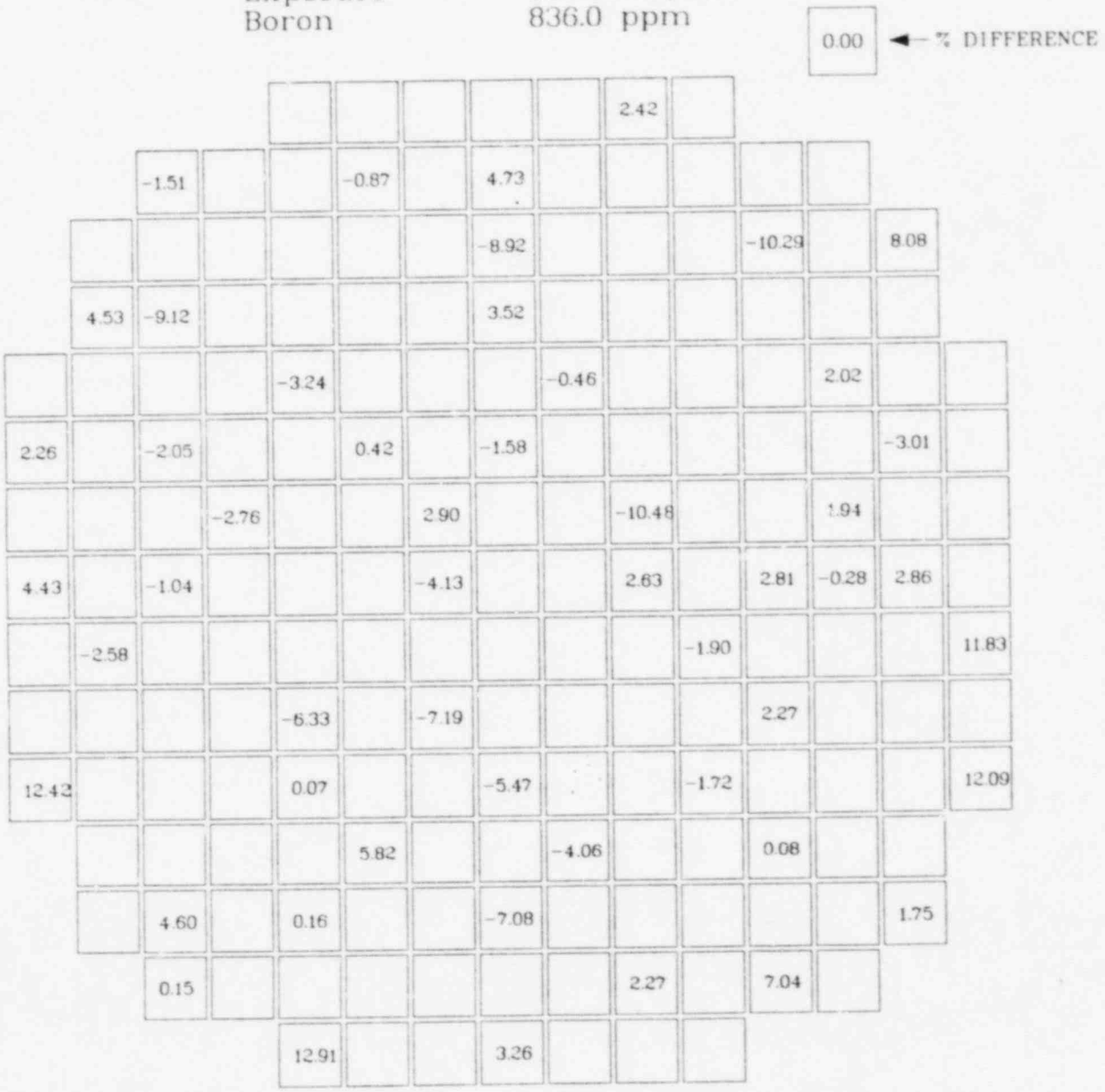

Fig. 4.17 Measured/Calculated Detector Response Factor

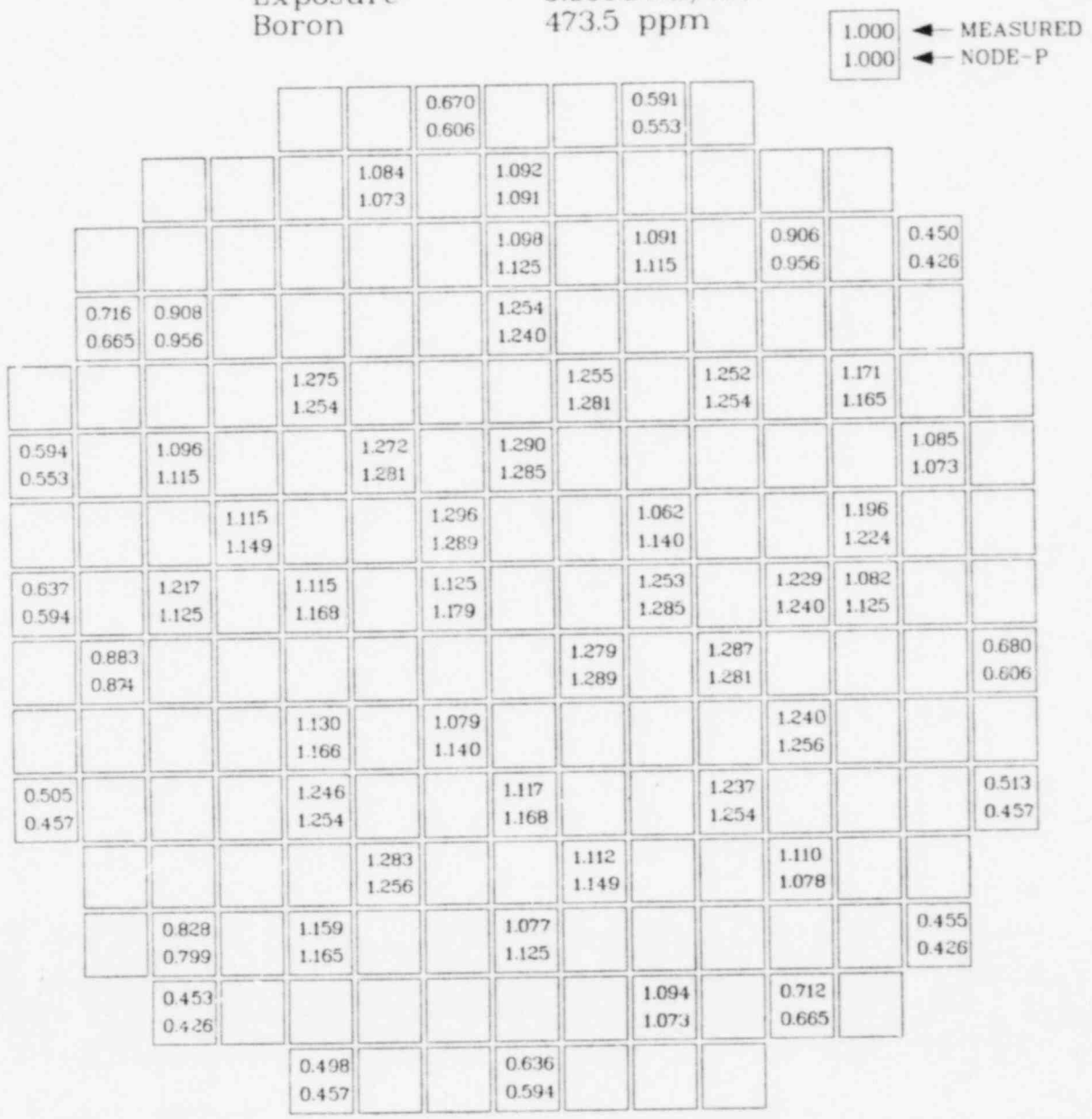

Fig. 4.18 Difference In
Measured/Caiculated Detector Response Factor

Exposure 9.099GWD/MT
Boron 473.5 ppm

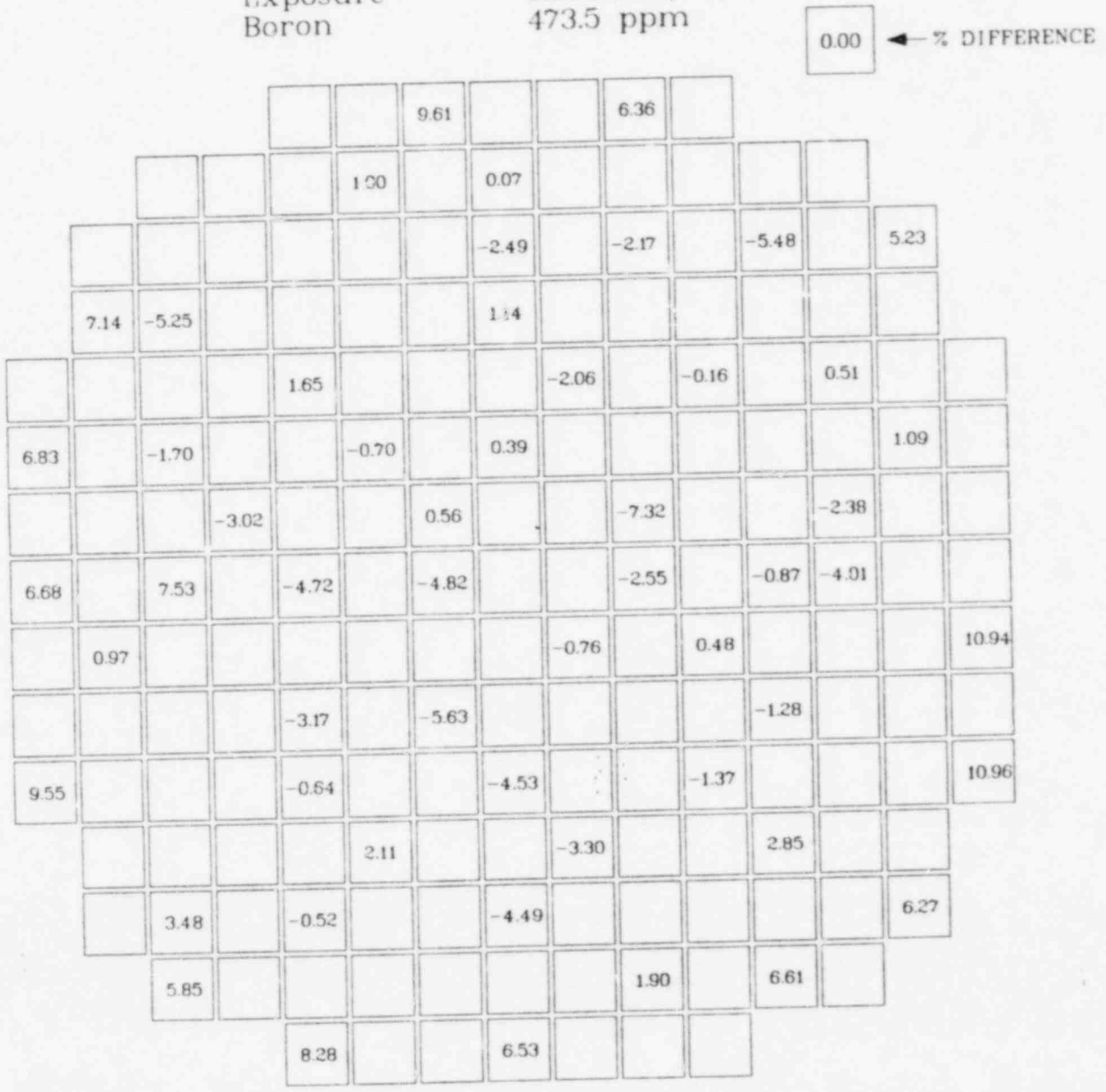

Fig. 4.19 Measured/Calculated Detector Response Factor

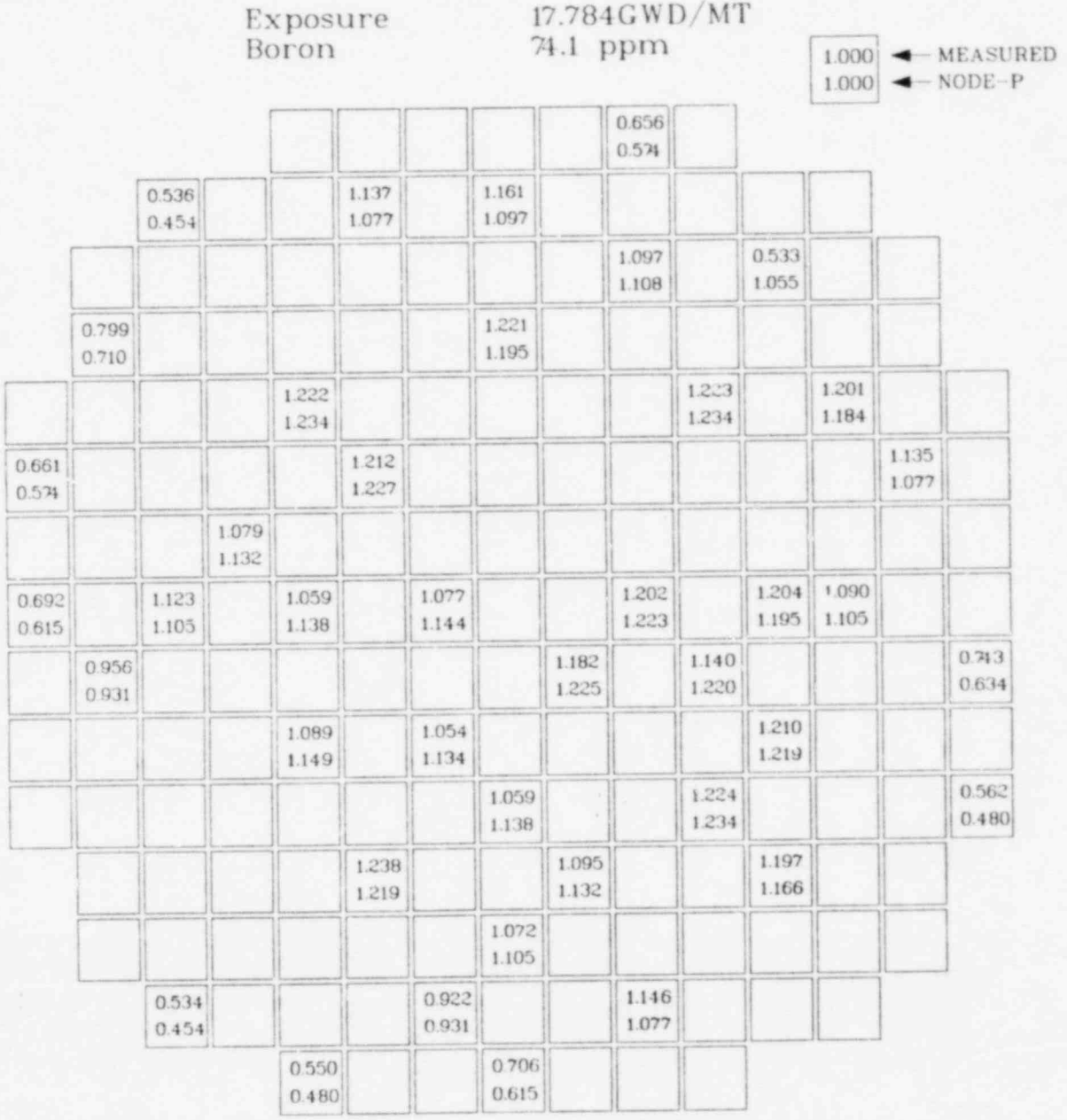

Fig. 4.20 Difference In
Measured/Calculated Detector Response Factor

Exposure 17.784GWD/MT
Boron 74.1 ppm

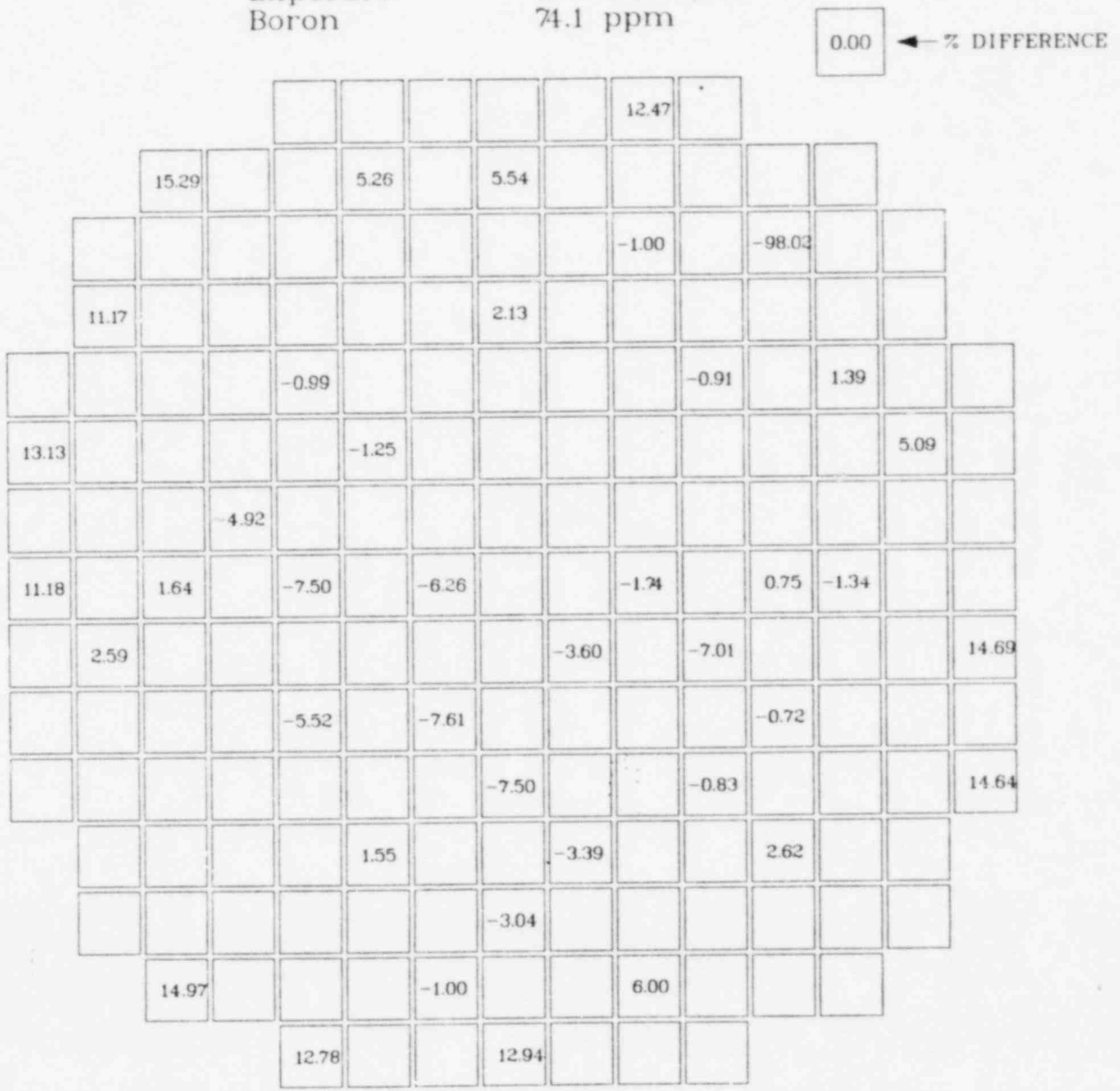

Fig. 4.21 CORE AVERAGE AXIAL POWER DISTRIBUTION
ZION-2. CY-1 - EXPOSURE 53. MWD/T

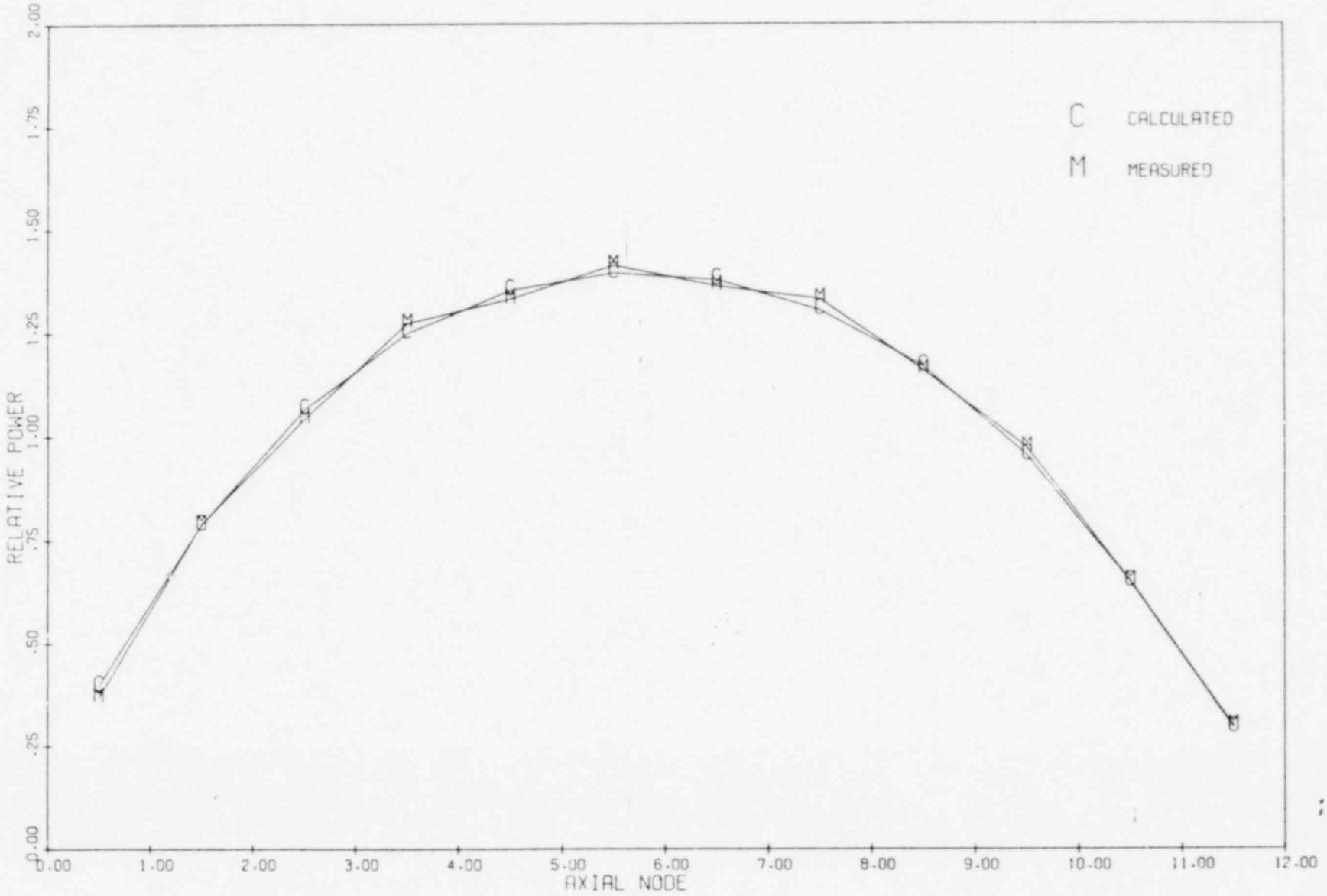

Fig. 4.22 CORE AVERAGE AXIAL POWER DISTRIBUTION
ZION-2. CY-1 - EXPOSURE 1602. MWD/T

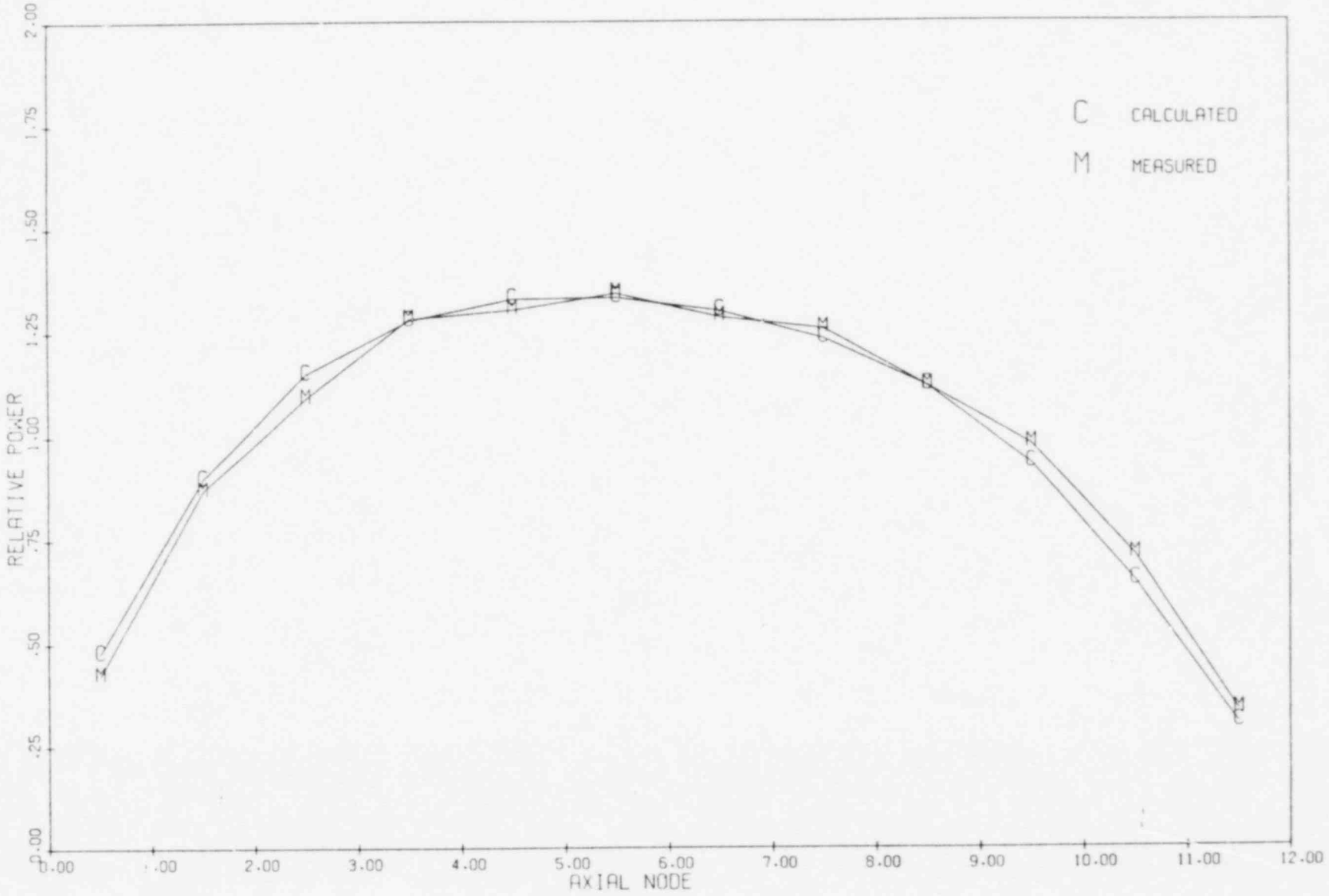

Fig. 4.23 CORE AVERAGE AXIAL POWER DISTRIBUTION
ZION-2, CY-1 - EXPOSURE 9099. MWD/T

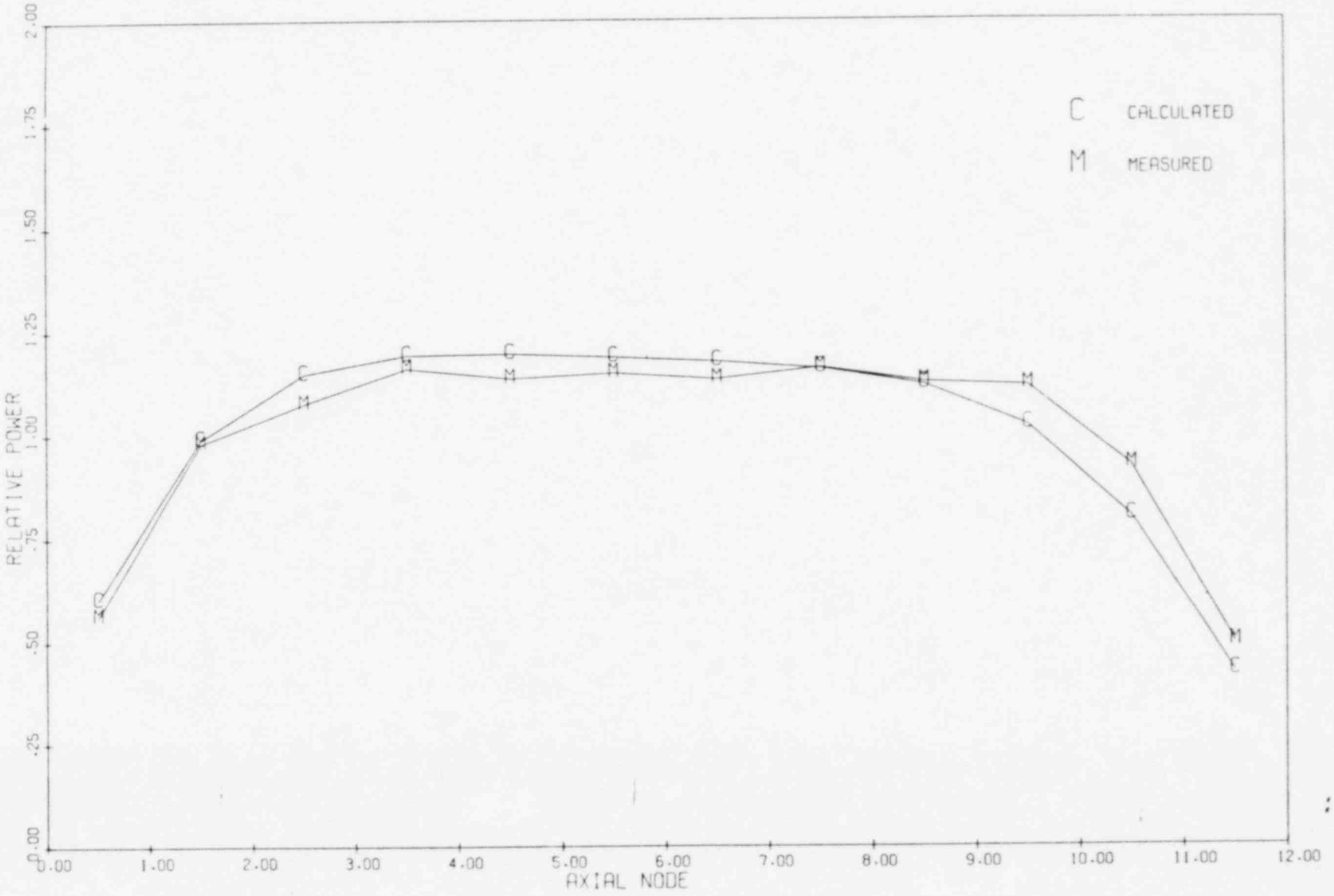

Fig. 4.24 CORE AVERAGE AXIAL POWER DISTRIBUTION
ZION-2, CY-1 - EXPOSURE 17784.MWD/T

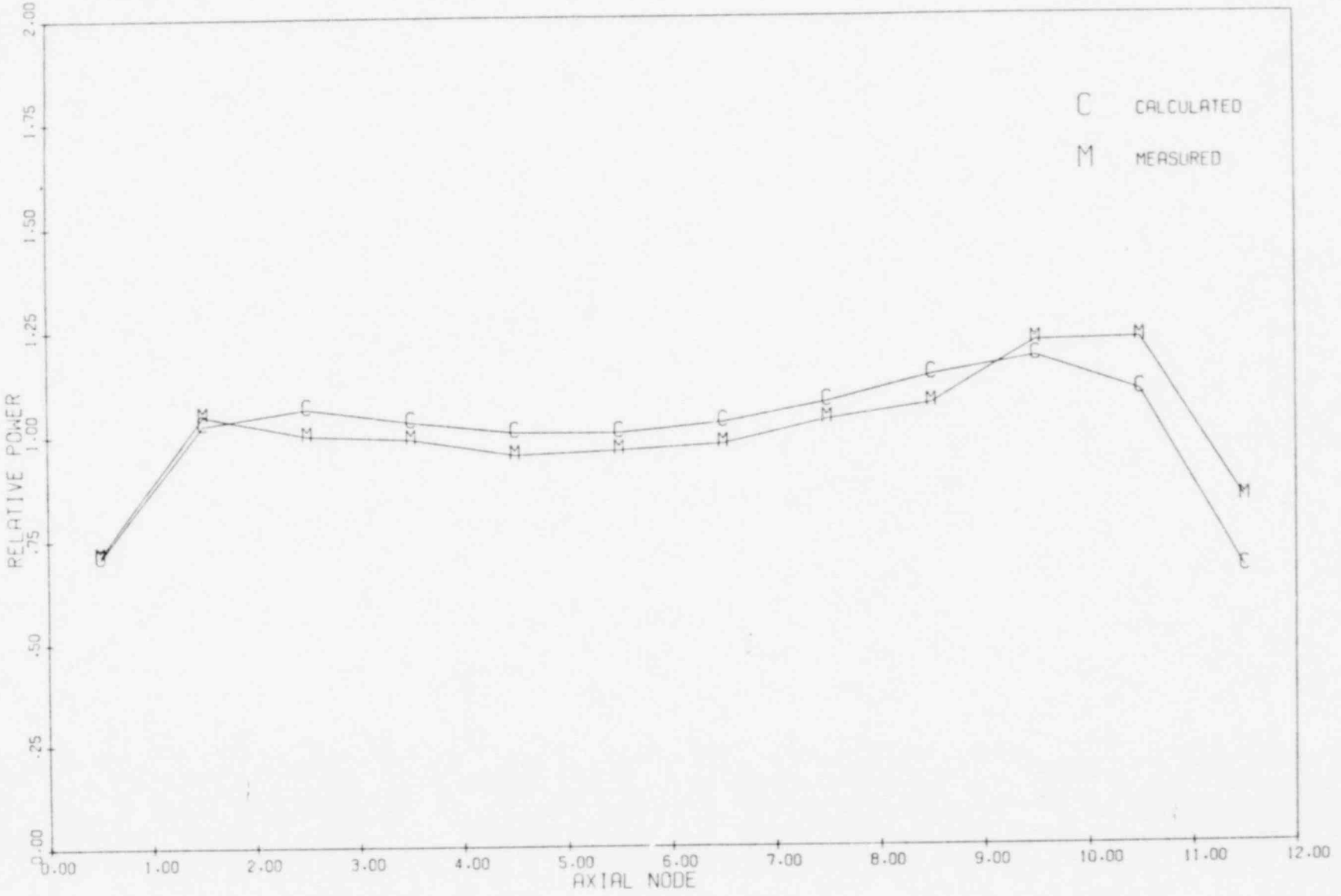

APPENDIX-A

Comparison Between 15x15 and 17x17 Fuel Assemblies

In this Appendix a comparison is presented between the 15x15 and 17x17 W optimized fuel assemblies. The purpose of this analysis was to compare the important assembly parameters required for the three-dimensional NODE-P calcualtions, such as k_∞, M^2 and various spectral coefficients. In summary one can conclude that based on the very similar neutronic behavior of the 15x15 and 17x17 fuel assemblies, the validity of the results presented in this report for the Zion Unit 2 core can be extended to other reactors loaded with 17x17 fuel types.

For simplicity two 15x15 fuel assembly types from the Zion Unit 2 core were compared with similar (17x17) types from the Byron & Braidwood units. Table A-1 lists the various characteristics of these fuel assemblies. Both reactor cores contained other types of bundles, mainly differing in the number of BPR's present. Peripheral bundles were not analyzed. The assembly burnup and BOL calculations were performed with the transport theory code, CASMO. Figures A-1 through A-4 show the essential results of the analysis, k_∞ and M^2 vs. exposure. For both fuel types the k_∞ and M^2 values are very similar with the maximum deviations of less than ~2 percent.

For completeness Fig. A-5 and A-6 show the ratio of ϕ_1/ϕ_2 indicating the similarities in the spectrum with the maximum deviation of less than ~10% at 40 GWD/MT.

Table A-2 lists the Doppler and boron coefficients in the form of the corresponding "B"- constants, and the k_∞ and M^2 temperature dependence is also indicated. It can be seen that both fuel types (15x15 and 17x17) have a very similar neutronic behavior with respect to parameters essential for the three-dimensional calculations.

TABLE A-1 - Comparison of Fuel Assembly Data

	Fuel Type 1		Fuel Type 2	
	Zion Unit 2	Byron & Braidwood	Zion Unit 2	Byron & Braidwood
Enrichment w/o U^{235}	2.25	2.10	2.79	2.60
Geometry	15x15	17x17	15x15	17x17
# Fuel Rods	204	264	204	264
Fuel Rod Pitch, in.	.563	.496	.563	.496
Instrument Location	1	1	1	1
Water Rods	20	24	0	0
BPR	0	0	20	24
Fuel Pellet Mat./ Dens. g/cm^3	UO_2/10.28	UO_2/10.41	UO_2/10.17	UO_2/10.41
Clad Mat./Dens., g/cm	Zr-4/1.284	Zr-4/*	Zr-4/1.284	Zr-4/*
Clad O.D./I.D, cm	1.072/.9486	.950/.836	1.072/9486	.950/.836
Guide Tube Mat.	Zr-4	Zr-4	Zr-4	Zr-4
Guide Tube O.D/ I.D., cm	1.384/1.308	1.224/1.144	1.384/1.308	1.224/1.144
BPR Material	-	-	Borosilicate Glass	Borosilicate Glass
B_2O_3 W/O % (B^{-10})	-	-	17.0	12.5
Clad Mat.	-	-	SS304	SS304
Inner Clad O.D/ I.D., cm	-	-	0.601/.568	.458/*
Outer Clad O.D./ I.D., cm	-	-	1.116/1.017	.968/*

* Data Unavailable

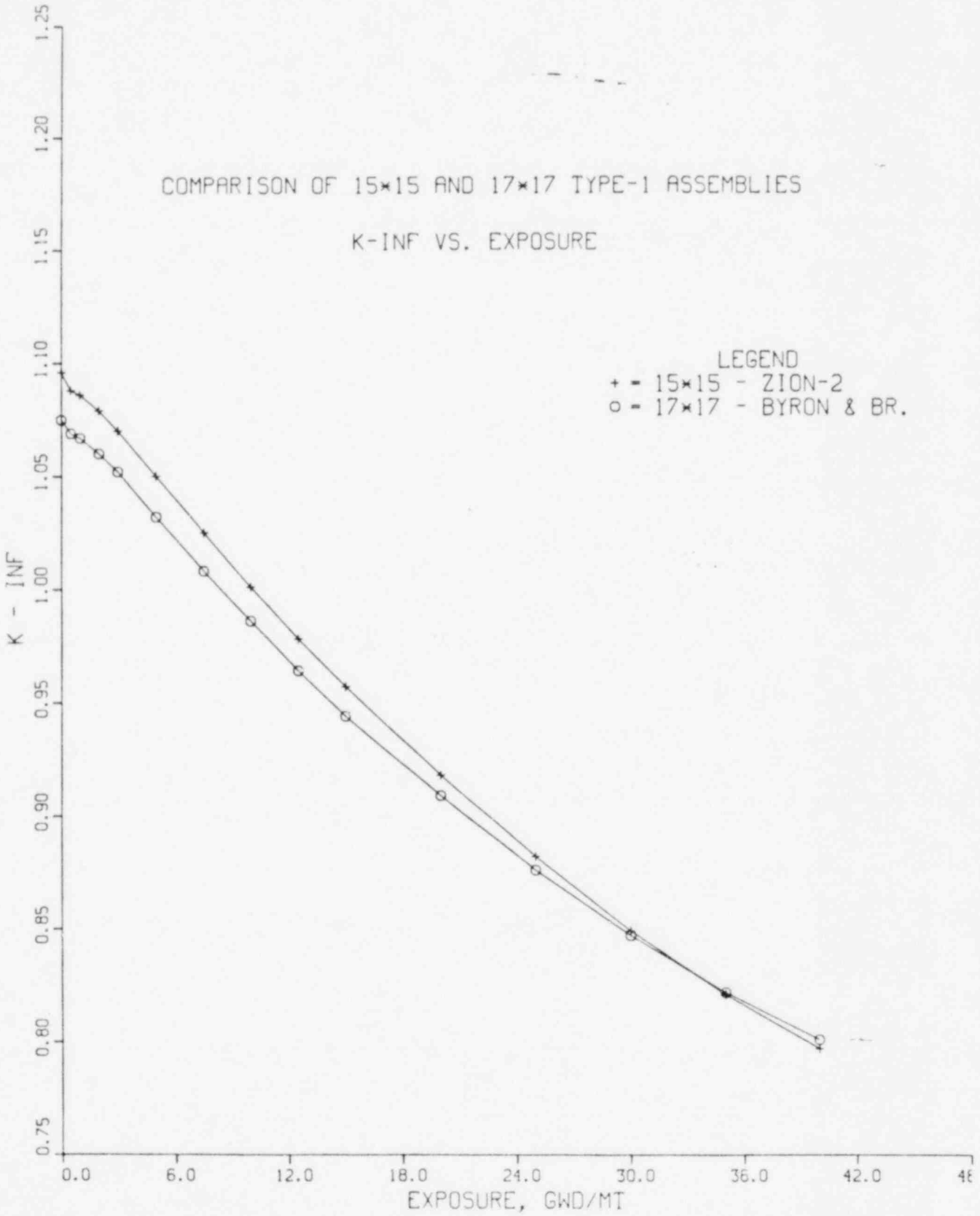

Figure A-1 Comparison of k_∞ vs. Exposure - Type 1 Fuel

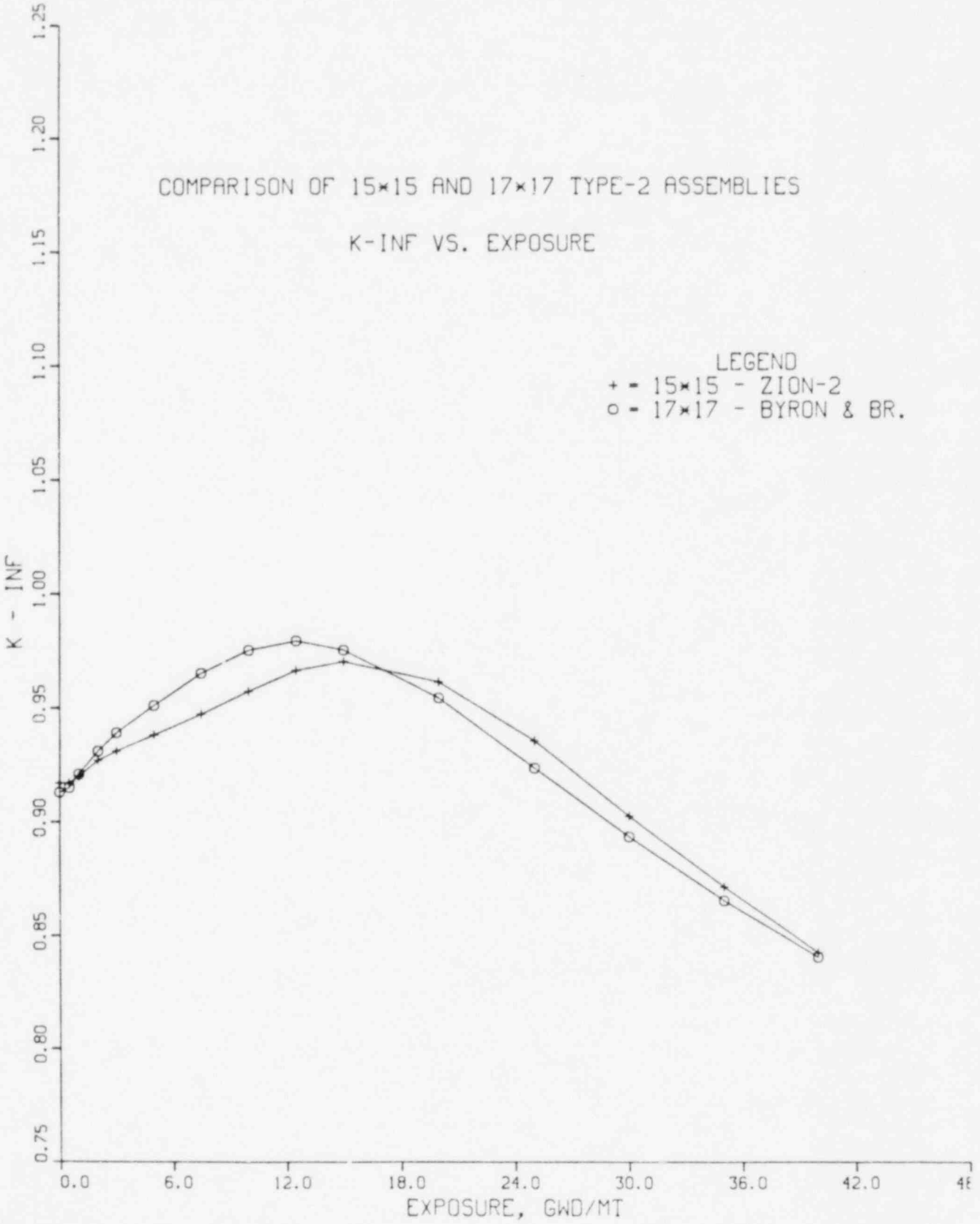

Fig. A-2 Comparison of k_∞ vs. Exposure - Type 2 Fuel

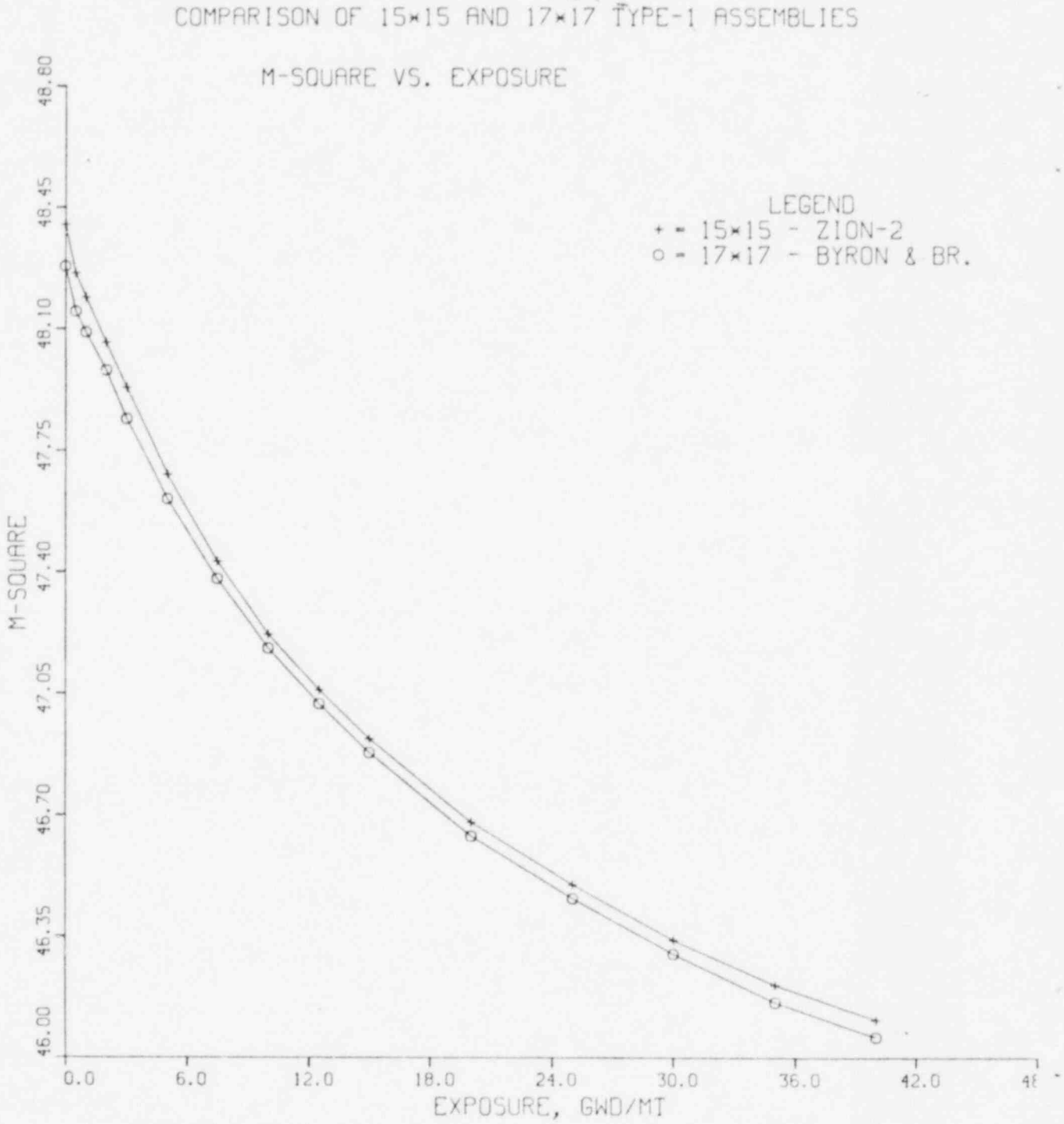

Fig. A-3 Comparison of M^2 vs. Exposure - Type 1 Fuel

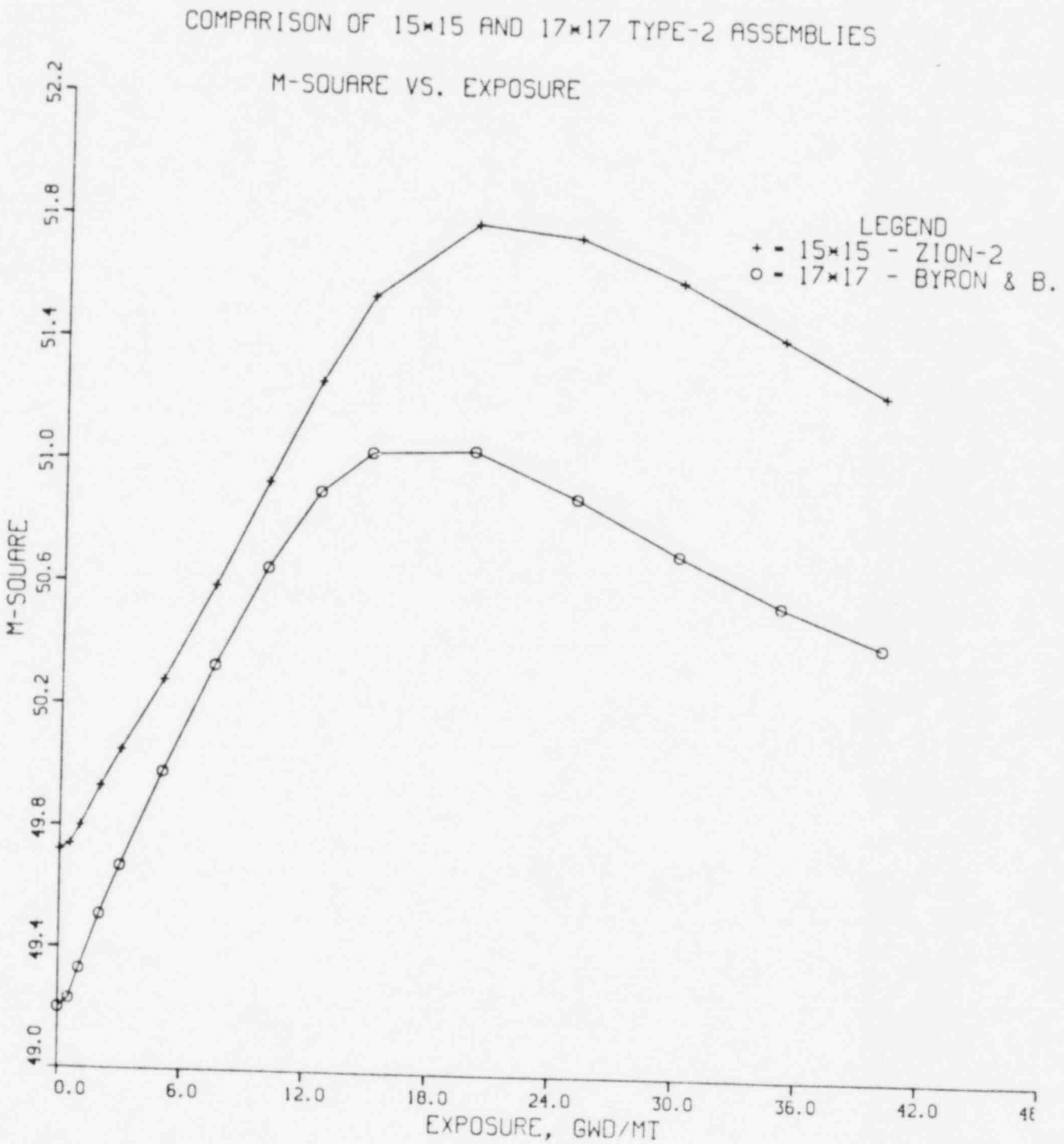

Figure A-4 Comparison of M^2 vs. Exposure - Type 2 Fuel

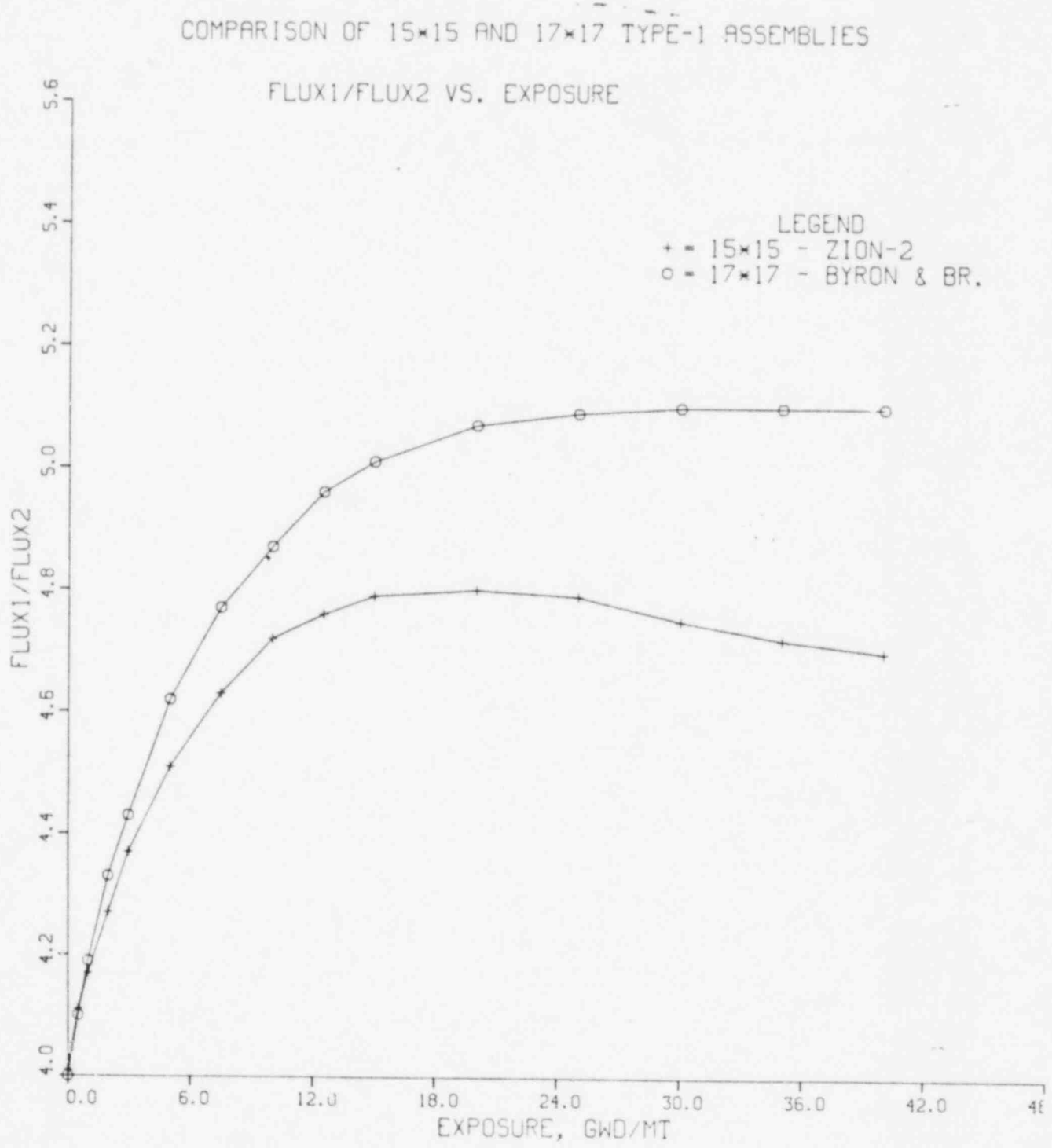

Figure A-5 Comparison of ϕ_1 / ϕ_2 Exposure - Type 1 Fuel

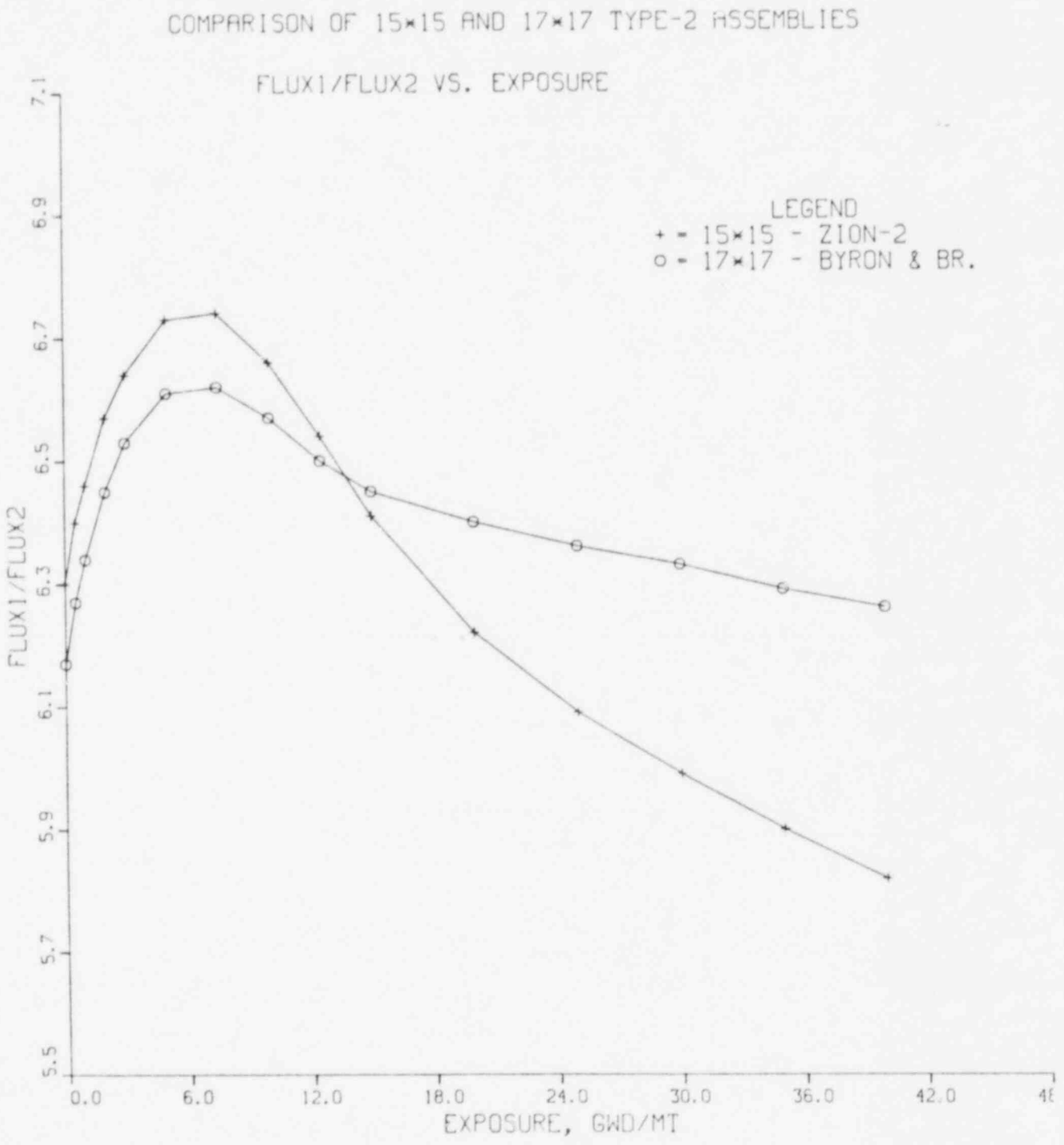

Figure A-6 Comparison of ϕ_1 / ϕ_2 vs. Exposure - Type 2 Fuel

TABLE A-2
Comparison Of 15x15 And 17x17 Fuel Assembly Coefficients

Coefficient	Equation	Fuel Type 1		Fuel Type 2	
		Zion Unit 2	Byron & Braidwood	Zion Unit 2	Byron & Braid
Doppler	$B_{17} = I_{fuel}$	.15474-02	.16620-02	.18722-02	.19803-02
Boron Worth	$B_{21} = N_B$	.24762+05	.25114+05	.18637+05	.18745+05
k_∞ vs. Temp.	k^1 (T_1 = 535°K)	1.25434	1.23103	1.00950	1.00519
	k^2 (T_2 = 560°K)	1.24887	1.22717	.99898	.99541
	k^3 (T_3 = 600°K)	1.23371	1.20928	.97511	.97306
M^2 vs. Temp.	M^2 (T_1 = 555°K)	43.948	44.095	46.042	45.574
	M^2 (T_2 = 560°K)	47.316	47.435	49.250	48.730
	M^2 (T_3 = 600°K)	56.130	56.154	57.580	56.894

Note: Calculations were done at BOL, HZP, 0 PPM Boron

APPENDIX-B

The B-Constants

Lists of the B-constants for the nine different fuel types are given in Table B-1 through B-3.

The change in k_∞ due to burnup, $\Delta\rho(E)$ is fitted as a function of exposure with coefficients B_{33}, B_{35}, B_{36}, B_{37}, and B_{54}. We have found that a 4th order polynomial fitted through the whole exposure range would give rather large errors at low exposure. Therefore, two intervals were chosen (0-3 MWd/kg U and 3-30 MWd/kgU) and $\Delta\rho(E)$ was fitted with two separate polynomials. Each of the polynomials were valid in their respective intervals only. Table B-1 through B-3 list the coefficients of the polynomial valid in the range 0-3 MWd/kgU. Table B-4 lists the coefficients for the interval 3-30 MWd/kgU.

It was also found that Xe dependence on exposure was rather weak and by setting $B_{16}=0$ the maximum error in Xe through the whole exposure range is less than 1.8%. B_{43} was determined by hand calculations using extra CASMO runs not required for SUPERLINK-P (moderator temperature reactivity). The control rod worth is represented by a polynomial with coefficients B_{55} through B_{58}. These constants were also hand calculated, since SUPERLINK-P generated only first order dependence of $\Delta\rho$ rod (B_{31} and B_{32}).

TABLE B-1 "B"-Constants for Region 3

FUEL TYPE 1
ENRICHMENT = 2.24%
NO. OF BPR = 0

"B" CONST.					
1-5	.12455E+03	-.37075E+03	.42704E+03	.73896E+00	.92227E+00
6-10	.11056E+01	.97190E+00	.75701E+00	.61338E+00	-.12892E+01
11-15	-.92851E+00	-.68746E+00	.97846E+00	.15526E+08	.14775E+07
16-20	0.	.15475E-02	.54860E+03	.12830E+04	0.
21-25	.24762E+05	-.94647E-02	.99149E+01	.11409E+00	-.52642E-02
26-30	.12021E+00	.23624E-02	-.83794E-04	-.12193E+00	-.52747E-01
31-35	0.0	0.0	.26579E-01	0.	-.25059E-01
36-40	.11946E-01	-.18426E-02	.58041E-03	0.	0.
41-45	0.	1.0	0.33733E-01	0.99774E+00	0.0
46-50	0.	0.	0.0	0.0	0.0
51-55	0.0	0.0	0.0	.11102E-15	1.00179E+00
56-60	-.91663E-02	1.0426E-03	-.19011E-04	0.	0.

FUEL TYPE 5
ENRICHMENT = 2.78%
NO. OF BPR = 0

"B" CONST.					
1-5	.11845E+03	-.35162E+03	.40513E+03	.78970E+00	.96921E+00
6-10	.11487E+01	.99264E+00	.79296E+00	.65569E+00	-.12984E+01
11-15	-.96875E+00	-.74214E+00	.98409E+00	.13060E+08	.14278E+07
16-20	0.	.14103E-02	.54860E+03	.12830E+04	0.
21-25	.20499E+05	-.47526E-02	.12070E+02	.80802E-01	-.50622E-02
26-30	.14623E+00	.19106E-02	-.79332E-04	-.12193E+00	-.52747E-01
31-35	0.0	0.0	.26026E-01	0.	-.23084E-01
36-40	.10659E-01	-.16205E-02	.46564E-03	0.	0.
41-45	0.	1.0	0.35158E-01	1.00853	0.
46-50	0.	0.	0.0	0.0	0.0
51-55	0.0	0.0	0.0	0.0	1.00178E+00
56-60	-.43478E-02	0.77134E-03	-.13350E-04	0.	0.

FUEL TYPE 10
ENRICHMENT = 3.29%
NO. OF BPR = 0

"B" CONST.					
1-5	.11923E+03	-.35370E+03	.40740E+03	0.	0.
6-10	.11804E+01	0.	0.	.67540E+00	0.
11-15	0.	-.76869E+00	0.	.11364E+08	.13864E+07
16-20	0.	.13197E-02	.54860E+03	.12830E+04	0.
21-25	.17893E+05	-.20829E-02	.13899E+02	.56155E-01	-.48766E-02
26-30	.16832E+00	.15610E-02	-.75283E-04	-.12193E+00	-.52747E-01
31-35	0.	0.0	.24538E-01	0.	-.20762E-01
36-40	.93303E-02	-.13990E-02	.39673E-03	0.	0.
41-45	0.	1.0	0.28909E-01	0.99388	0.
46-50	0.	0.	0.0	0.0	0.0
51-55	0.0	0.0	0.0	.22204E-16	0.
56-60	0.	0.	0.	0.	0.

TABLE B-2 "B"-Constants For Region 2

FUEL TYPE 2
ENRICHMENT = 2.78%
NO. OF BPR = 20

"B" CONST.					
1-5	.10919E+03	-.31144E+03	.36034E+03	0.	0.
6-10	.89662E+00	0.	0.	.71885E+00	0.
11-15	0.	-.93101E+00	0.	.11656E+08	.14158E+07
16-20	0.	.18716E-02	.54860E+03	.12830E+04	0.
21-25	.18637E+05	-.15415E-01	.13098E+02	.15253E+00	-.74316E-02
26-30	.15904E+00	.29953E-02	-.11420E-03	-.12193E+00	-.52747E-01
31-35	0.	0.0	.11717E-01	0.	-.23257E-01
36-40	.11089E-01	-.16995E-02	.85462E-03	0.	0.
41-45	0.	1.0	-.21392E-01	1.00853E+00	1.0
46-50	0.	0.	0.0	0.0	0.0
51-55	0.0	0.0	0.0	.55511E-16	0.
56-60	0.	0.	0.	0.	0.

FUEL TYPE 3
ENRICHMENT = 2.78%
NO. OF BPR = 16

"B" CONST.					
1-5	.11198E+03	-.32186E+03	.37208E+03	0.	0.
6-10	.93647E+00	0.	0.	.72268E+00	0.
11-15	0.	-.91855E+00	0.	.12139E+08	.14186E+07
16-20	0.	.17812E-02	.54860E+03	.12830E+04	0.
21-25	.19084E+05	-.13226E-01	.12824E+02	.13709E+00	-.69072E-02
26-30	.15564E+00	.27566E-02	-.10640E-03	-.12193E+00	-.52747E-01
31-35	0.	0.0	.149330E-01	0.	-.23298E-01
36-40	.11053E-01	-.16960E-02	.77061E-03	0.	0.
41-45	0.	1.0	-.18994E-01	1.00853E+00	1.0
46-50	0.	0.	0.0	0.0	0.0
51-55	0.0	0.0	0.0	.11102E-15	0.
56-60	0.	0.	0.	0.	0.

FUEL TYPE 4
ENRICHMENT = 2.78%
NO. OF BPR = 12

"B" CONST.					
1-5	.11610E+03	-.33642E+03	.38858E+03	0.	0.
6-10	.98150E+00	0.	0.	.71053E+00	0.
11-15	0.	-.88532E+00	0.	.12423E+08	.14211E+07
16-20	0.	.16913E-02	.54860E+03	.12830E+04	0.
21-25	.19506E+05	-.11164E-01	.12573E+02	.12153E+00	-.63934E-02
26-30	.15252E+00	.25203E-02	-.98839E-04	-.12193E+00	-.52747E-01
31-35	0.	0.0	.17830E-01	0.	-.23141E-01
36-40	.10837E-01	-.16509E-02	.69914E-03	0.	0.
41-45	0.	1.0	-.15041E-01	1.00853E+00	1.0
46-50	0.	0.	0.0	0.0	0.0
51-55	0.0	0.0	0.0	.11102E-15	0.
56-60	0.	0.	0.	0.	0.

Table B-3 "B" - Constants for Fuel Assemblies
Without BPR

FUEL TYPE 6
ENRICHMENT = 3.29%
NO. OF BPR = 20

"B" CONST.					
1-5	.11115E+03	-.31650E+03	.36626E+03	0.	0.
6-10	.93830E+00	0.	0.	.73404E+00	0.
11-15	0.	-.93921E+00	0.	.10040E+08	.13662E+07
16-20	0.	.17190E-02	.54860E+03	.12830E+04	0.
21-25	.15934E+05	-.11529E-01	.15433E+02	.12451E+00	-.72005E-02
26-30	.18730E+00	-.26253E-02	-.10974E-03	-.12193E+00	-.52747E-01
31-35	0.	0.0	.14309E-01	0.	-.20702E-01
36-40	.93519E-02	-.13903E-02	.71789E-03	0.	0.
41-45	0.	1.0	-.12481E-01	0.99388E+00	1.0
46-50	0.	0.	0.0	0.0	0.0
51-55	0.0	0.0	0.0	.27756E-16	0.0
56-60	0.	0.	0.	0.	0.

FUEL TYPE 7
ENRICHMENT = 3.29%
NO. OF BPR = 12

"B" CONST.					
1-5	.11551E+03	-.33399E+03	.38585E+03	0.	0.
6-10	.10197E+01	0.	0.	.73213E+00	0.
11-15	0.	-.90446E+00	0.	.10503E+08	.13707E+07
16-20	0.	.15635E-02	.54860E+03	.12830E+04	0.
21-25	.16702E+05	-.78019E-02	.14800E+02	.97733E-01	-.62450E-02
26-30	.17946E+00	-.22036E-02	-.95504E-04	-.12193E+00	-.52747E-01
31-35	0.	0.0	.18752E-01	0.	-.20831E-01
36-40	.94076E-02	-.14078E-02	.58506E-03	0.	0.
41-45	0.	1.0	-.05448E-01	0.99388E+00	1.0
46-50	0.	0.	0.0	0.0	0.0
51-55	0.0	0.0	0.0	.55511E-16	0.
56-60	0.	0.	0.	0.	0.

FUEL TYPE 8
ENRICHMENT = 3.29%
NO. OF BPR = 8

"B" CONST.					
1-5	.11624E+03	-.33880E+03	.39108E+03	0.	0.
6-10	.10681E+01	0.	0.	.72446E+00	0.
11-15	0.	-.87478E+00	0.	.10731E+08	.13756E+07
16-20	0.	.14815E-02	.54860E+03	.12830E+04	0.
21-25	.17048E+05	-.60977E-02	.14542E+02	.85112E-01	-.58158E-02
26-30	.17626E+00	-.20071E-02	-.89109E-04	-.12193E+00	-.52747E-01
31-35	0.	0.0	.21014E-01	0.	-.20851E-01
36-40	.93798E-02	-.14024E-02	.52764E-03	0.	0.
41-45	0.	1.0	0.00094E+00	0.99388E+00	1.0
46-50	0.	0.	0.0	0.0	0.0
51-55	0.0	0.0	0.0	.55511E-16	0.
56-60	0.	0.	0.	0.	0.

TABLE B-4 "B"-Constants
Cofficients Of $\Delta\rho$ (E)
In Region 3-30 MWd/kgU

Fuel Type	1	2	3	4	5	6	7	8	10
B_{33}	.89341-02	.39298-03	.23288-02	.40247-02	.80153-02	.82975-03	.37196-02	.50897-02	.71094-02
B_{35}	.45760-04	-.70107-03	-.59498-03	-.47997-03	.57221-04	-.37216-03	-.23393-03	-.13550-03	.72606-04
B_{36}	-.46818-05	.38618-04	.31660-04	.24907-04	-.49370-05	.15624-04	.85624-05	.33684-05	-.53214-05
B_{37}	.87144-07	-.50271-06	-.40478-06	-.31601-06	.96955-07	-.10826-06	-.37294-07	.24803-07	.10291-06
B_{54}	.38513-03	-.82813-02	-.62923-02	-.43028-02	.24196-02	-.30531-02	-.53181-03	.89943-03	.35056-02

DISTRIBUTION LIST

U.S. Nuclear Regulatory Commission

H. Denton
W. Dircks
M. Dunenfeld (2)
S. Fabic
D. Fieno (7)
W. Johnson
L. Lois
R. Mattson
R. Minogue
L. Rubenstein

Advisory Committee Reactor Safeguards (16)
Bethesda Technical Library
Director, Office of Standards Development
Public Document Room
Technical Assistant, Executive Director's Office

Brookhaven National Laboratory

Core Performance Group
Core and Systems Code Development Group
DNE Associate & Deputy Chairmen
Nuclear Safety Group Leaders

External

T. Anderson, W
D. Bell, EPSC
M. Edenius, Studsvik
W. Eich, EPRI
S. Hartzell, UCC
E. Lanning, EPRI
G. Lellouche, EPRI
R. Mills, C-E
R. Mosteller, S. Leavy Assoc.
C. Owsley, ENC
G. Sherwood, GE
J. Taylor, B&W

PDR

INTERIM REPORT

NRC Research and/or Technical Assistance Report

Accession No. _____

Contract Program or Project Title: Core Performance

Subject of this Document: Simulation of Zion Unit 2 Cycle-1 Operation

Type of Document: Informal

Author(s): P. Kohut, D. Cokinos, J. Carew

Date of Document: April 1982

Responsible NRC Individual and NRC Office or Division:
Mr. Marvin Dunenfeld
Division of Systems Integration
U.S. Nuclear Regulatory Commission
Washington, D.C. 20555

Brookhaven National Laboratory
Upton, NY 11973
Associated Universities, Inc.
for the
U.S. Department of Energy

Prepared for
U.S. Nuclear Regulatory Commission
Washington, D. C. 20555
Under Interagency Agreement EY-76-C-02-0016
NRC FIN No. A-

INTERIM REPORT